Research Article

Yunyang Wang*, Liqing Zhang*, and Shengwei Sun

Cementitious composites modified by nanocarbon fillers with cooperation effect possessing excellent self-sensing properties

https://doi.org/10.1515/ntrev-2023-0226
received November 26, 2023; accepted February 21, 2024

Abstract: The safety and durability of concrete structures are prone to damage and result in significant harm to human society. Hence, monitoring and estimating the states of concrete structures is of great significance to protecting human safety. Graphene nanoplatelets (GNPs) and carbon nanotubes (CNTs) are promising candidates to endow cementitious composites with piezoresistivity for the health monitoring of concrete structures. Therefore, the aim of this article is to explore the effect of the hybrid GNPs and CNTs on behavior of cementitious composites with cooperation effects. The cementitious composites containing the hybrid GNPs and CNTs with simplified manufacturing methods are developed first. And then, the mechanical behaviors, electrical conductivities, and piezoresistive performances of the composites are investigated systematically. Finally, the modification mechanisms are also discussed. The results proved that the electrical resistivity of the composites with the hybrid GNPs and CNT concentration of 5.0 wt% is reduced by three orders of magnitudes, and the FCR and sensitivities are reached at 36.0% and 1.1% MPa^{-1}/177.9, respectively. Its compressive strength/elastic modulus is achieved at 73.3 MPa/16.9 GPa. Therefore, the hybrid GNPs and CNTs modified cementitious composite present great potential application in monitoring and evaluating service states of civil infrastructures.

Keywords: nanocarbon materials, cementitious composites, self-sensing properties

*** Corresponding author: Yunyang Wang,** School of Civil Engineering and Architecture, Hunan University of Arts and Science, Changde 415000, China, e-mail: hnwangyunyang@126.com, tel: +86-15211204091
*** Corresponding author: Liqing Zhang,** School of Civil Engineering and Architecture, East China Jiaotong University, Nanchang 330013, China; Zhongheng Construction Group Co., Ltd, Nanchang 330200, China, e-mail: zlq@ecjtu.edu.cn
Shengwei Sun: China Construction Second Engineering Bureau Co., Ltd, Beijing 100160, China

1 Introduction

Large quantities of civil infrastructures have been built using concrete globally each year, such as buildings, roads, bridges, and dams for good durability, high compressive strength, and economy [1–5]. However, various types of loads, aggressive environmental effects, and aging will lead to damages, cracks, and premature degradation of concrete structures; thus, their safety and durability will be reduced and even cause disasters [2,6]. Therefore, health monitoring of concrete structures by detecting and evaluating the performances from measuring deformations, stress, strains, cracks, and temperature by sensory systems in real time is of great significance based on the crucial demands of sustainable civil infrastructures. It also makes a contribution to developing smart, economical, and environmentally friendly civil infrastructures [7,8].

Traditional sensing technical applied in monitoring and evaluating working states of concrete structures include optical fibers, accelerometers, strain gauges, and vibrating wires. However, these sensors possess disadvantages such as low durability and authenticity, not compatible with cementitious composites, and costly. Thus, their application is limited [9,10]. Cementitious composites possessing sensing behaviors constitute electrically conductive fillers and cementitious composites, which combine sensing properties and structure functions and can detect and monitor working states at the actual time. The composites were developed first by Chung in the 1990s [11], possessing great sensing and mechanical behaviors; thus, they are attracted to prepare smart materials and structures in civil infrastructures. Therefore, self-sensing cementitious composites possess huge potential in monitoring and evaluating the health of civil infrastructures for their outstanding performances [6,12].

Commonly used electrical conductive fillers including steel fibers [13,14], carbon fibers (CFs) [15–17], carbon nanotubes (CNTs) [18], nickel powders [9,19–22], metal oxides [14], carbon blacks (CBs) [23–25], and graphene nanoplatelets (GNPs) [3]. However, the electrical conductivities of the

steel fibers, nickel powders, and metal oxides are prone to be affected by environmental factors. Thus, the stability and accuracy of the sensing performances of cementitious composites including these electrical conductive fillers will be affected [13]. Nevertheless, the electrically conductive fillers of nanocarbon materials present good alkali prevention, excellent durability, and electrical conductive performances, which are considered to be ideal electrical conductive fillers for cementitious composites [15,18].

GNPs consist of carbon atoms that are tightly bound and possess two-dimensional sheet-like structures. They possess an extremely thin nuclear thickness of only a few nanometers and have multiple layers like a honeycomb structure. The tensile strength is more than 130 GPa as well as Young's modulus is higher than 1.0 TPa. Meanwhile, their electrical conductivity is 1.0×10^6 higher than that of copper [26–28]. Thus, cementitious composites can be endowed with excellent piezoresistive response, and mechanical behaviors as well as electrical conductivity also can be improved for the remarkable features of GNPs. Therefore, applying the GNPs in prepared cementitious composites with outstanding sensing performances is drawing increasing concentrations [29,30]. Le *et al.* manufactured GNPs cementitious composites and studied the relations between electrical resistivity and damage degree withstand shear load. However, the GNPs used as electrically conductive fillers are restricted due to the complicated preparation methods [31]. Sevim *et al.* revealed that GNPs can generate effective electrical conductive pathways and present good piezoresistivity with bigger particle sizes and lower surface areas [32]. The relations between damage and resistivity of cementitious composites containing GNPs withstand compressive load to failure indicate that the resistivity slightly falls within the elastic regime and then increases rapidly. The damages can be achieved at 0.8 accompanied by variation of the resistivities [33]. The self-sensing performances of the cementitious composites incorporating GNPs are not prone to be affected by humidity. Nevertheless, the composites display lower sensitivities at first but then increase and withstand higher compressive stress [34]. The gauge factor of GNP cementitious composites after penetrating in silane solutions can reach up to 141.8 and the composites also displayed great self-cleaning properties [35]. The resistivity of cementitious composites having the GNPs dosage of 6.4% display precise reaction to compression load. However, unstable piezoresistivity will be caused when the concentration of the GNPs is lower than 3.2% or higher than 12.8% [36]. The electrical resistivity of GNP cementitious composite sensors along axial, perpendicular, and slant directions subjected to compressive load can decrease by 5.5, 1.8 and 6.7%, respectively. The sensors can be embedded in a beam to detect the strains in different force state areas under bending, and the results are correlated well with the strain gauges [37]. Lu *et al.* adsorbed the GNPs on the sand surface as conductive aggregates and demonstrated that cementitious composite containing the conductive aggregates presents excellent electrical conductivity and piezoresistive effect with FCR reached up to 18% withstand circle compressive stress [38]. Dong *et al.* used silane coatings on the surface of GNP cementitious sensors and realized mitigated piezoresistive instability [39], they also demonstrated that the stabilized piezoresistivity of GNP cementitious composites incorporating 2% GNPs was well-maintained after impact [40].

CNTs are one-dimensional nanomaterials constituted of coaxial cylinder graphene layers, and their diameter and length are in nanometers and micrometers, respectively. The aspect ratio is even larger than 1,000 and with hollow structures, making it easy to provide electrically conductive pathways and networks within cementitious composites [41,42]. They are widely studied for improving the electrical and piezoresistive response of cementitious composites due to their stable chemical properties, remarkable mechanical performances, and excellent electrical conductivities and piezoresistive effect [43]. The resistivity of cementitious composites containing CNTs decreases upon increasing stress/strain to withstand compressive load [18]. Piezoresistivity performances are endowed owing to the formation of the electrically conductive pathways and networks within the cementitious composites, and their distribution is influenced by the water-to-binder ratios, curing and dry ways, specific area, agglomeration, and contents of the CNTs [44–47]. As demonstrated by Ramezani *et al.*, lower water-to-binder ratios can improve the distribution of the CNTs in cementitious composites. The mechanism is that the movements of the CNTs can be restricted due to the lower water-to-binder ratios, thus reducing re-agglomeration [48]. The contents of the CNTs corresponding to the optimal piezoresistivity are different under the different water-to-binder ratios [30,49–52]. Meanwhile, cementitious composites incorporating the CNTs not only present great self-sensing properties undergoing static compressive load, but also exhibit positive piezoresistivity to withstand dynamic load [53]. Additionally, the cracks of the concrete can also be detected by CNTs cementitious composites [49,54,55]. D'Alessandro *et al.* pointed out that the piezoresistivity of the CNTs cementitious composite sensors using a novel dispersant display higher sensitivities and linearity as well as reduced drift and hysteresis due to the dielectric nature can be decreased by the dispersant [56]. The piezoresistivity of the CNTs cementitious composites can be greatly improved by styrene-acrylic emulsion because of the three-dimensional networks structure, and the maximum stress sensitivity is reached up to 22.1×10^{-3} MPa^{-1} [57]. However, the CNTs are easy to agglomerate owing to

the strong Van der Waals force and high specific area. Additionally, the costly price is also the major limitation for CNTs applied in cementitious composites [58,59].

The challenges of using nano-electrical conductive fillers in cementitious composites include dispersion homogenous, and formation of the electrically conductive pathways and networks in the composites. The solutions to solve these challenges include ultrasonication, ball milling, and dry mix [60]. The mechanisms of the nano-electrical conductive filler's effect on the mechanical and electrical properties are as follows: (1) influence on the hydration products and prevent propagation of the crack; (2) improve the compactness; (3) enhance the distribution of the nano-electrical conductive fillers in cementitious composites, the bonding of the interfacial, and the efficiency on load-transfer; and (4) enhance the deposition of the hydration products and nucleation effect [60,61].

For the sake of solving the challenges encountered by the mono electrical conductive fillers, two or even more different kinds of electrical conductive fillers, named composite conductive fillers, have been explored to improve the self-sensing properties together. Composite conductive fillers can enable cementitious composites with superior self-sensing performances together with mechanical properties compared with the mono-electrical conductive fillers [62]. Additionally, the porous and defects can be filled and cracks can be bridged because of their vast aspect ratios and reasonable dimensions of the composite conductive fillers. Therefore, the electrical conductivity and sensitivities can be improved simultaneously. On the other hand, defects such as pores can be produced if the conductive fillers dispersion poorly, which will lead to decrease of strength. The diameter, content, and length of the conductive fillers are the key factors in determining the dispersion state [63].

Cementitious composites modified by CNTs together with CBs exhibit well self-sensing properties with stability together with repeatability, and better sensitivities mechanical performances [23,64]. Similarly, the CNTs and CFs can improve the sensitivities, reliability, and signal-to-noise ratio compared with the mono-CFs or CNTs because of CNTs can reduce the gaps between CFs conductively pathways for their different deformations [44,65]. Additionally, cementitious composites can be endowed with excellent self-sensing performances by CBs and GNPs with synergy effect [3]. The self-sensing and mechanical performances of cementitious composites can also be improved by CNTs and GNPs, and the stress/strain sensitivities and compressive strength is reached up to 0.49%/MPa/86.03 and 66.0 MPa, respectively, with the CNTs and GNPs dosage of 6.0 wt% [66]. Cementitious composites reinforced by carbon fibers and GNPs displayed considerable reversible piezoresistivity after prior drying process [67]. The cementitious composites show good detecting ability on strain, stress, and damage in elastic and plastic stages improved by the hybrid GNPs and CNTs with dosage from 3 to 4%. During the process of crack propagation and expansion, the FCR is increased, while it is decreased with shrinkage of cracks [68]. Liu *et al.* indicated that the FCR and gauge factor of nickel-coated CNTs cementitious composites is reached to 23.75% and 993, respectively, with content of the nickel-coated CNTs is 1.20 vol%. Additionally, the FCR and gauge factor reduced with increasing loading rate [69].

Recent studies in the nanotechnology field of construction have already used nanoparticles to enhance the electromechanical properties of cementitious composites, improving their quality and durability. The cementitious composites containing 0.2 wt% CNTs and 0.5 wt% CFs increased the conductivity by about 867 and 633%, respectively. This composite also presents the highest FCR under compressive cyclic loading compared with the cementitious composites incorporating the single CNTs or CFs. They implied that the distance decrease of the CNTs and CFs in the cementitious matrix formed a better network due to their synergy effect [70,71]. The self-sensing behaviors of the cementitious composites incorporating the hybrid carbon black and PP fibers subjected to bending, cyclic compression, and splitting tensile loads is comprehensively assessed by Guo *et al.* They pointed out that the improvement of the hybrid carbon black and PP fibers on electrical conductivity and self-sensing properties has relied on the coating effect of carbon black on the PP fiber surface [72].

Previous researches indicate that GNPs and CNTs are the most promising electrically conductive fillers for endowing cementitious composites with great piezoresistive characteristics owing to the superior properties, different dimensions, shapes, aspect ratios, and microstructures, as well as effective electrical conductive pathways and networks can be formed with higher efficiency within cementitious composites by cooperation effect [32,56,69,73–75]. However, limited studies are carried out on the GNPs together with CNTs effect on the performances of cementitious composites. Therefore, the simple preparation methods of cementitious composites modified by the hybrid GNPs and CNTs and their effect on the response of the composites is first explored in the present study. Then, mechanical performances, failure modes, and electrical resistivity are assessed. Thereafter, a monotonic and cyclic compressive load is applied to evaluate the piezoresistive behaviors. Moreover, mechanisms of cooperation effect of the hybrid GNPs and CNTs influence on properties of the composites are discussed comprehensively. The purpose of the present research is to overcome the issue of

uneven dispersion and low improving efficiency of single GNPs or CNTs, analyzing the improving effect of the hybrid GNPs and CNTs on behaviors of cementitious composites with cooperation effect.

2 Experimental process

2.1 Materials

Specifications of the hybrid GNPs and CNTs are shown in Table 1, and their typical scanning electron microscope (SEM) photos are displayed in Figure 1(a). As shown in Figure 1(a) that tube-shaped CNTs adhere to the surface of the GNPs, which possess the layered plate structures. The main production process of the hybrid GNPs and CNTs is as follows. The GNPs and CNTs are mixed in the solution with a mass ratio of 80 to 20%. Then, the solution was stirred evenly. After that, the solid and liquid of the solution was separated, and the separated solid was washed.

Table 1: The specifications of the hybrid GNPs and CNTs

Specifications	Values
Weight percentage of GNPs to CNTs	80 wt%: 20 wt%
Median size	5–7 μm
Resistivity	<0.15 Ω cm
Density	2.1 g cm^{-3}
Purity of GNPs	>90%
Diameter of GNPs	2–16 μm
Layers of GNPs	<3
Thickness of GNPs	5–60 nm
Purity of CNTs	>95%
Diameter of CNTs	30–80 nm
Length of CNTs	<10 μm
Special surface area of CNTs	220–300 m^2 g^{-1}/g

Finally, the obtained mixed GNPs and CNTs were dried and gridded. The density of Portland cement with a grade of 42.5 is 3.2 g/cm^3, and the density of fly ash is 2.3 g/cm^3. The hybrid GNPs and CNTs are easy to cluster and difficult to achieve good dispersion in the cementitious composites owing to the influence of van der Waals forces [76]. Therefore, a polycarboxylate superplasticizer containing 50% solid content is adopted to facilitate the hybrid GNPs and CNTs dispersion homogenously and to enhance the fresh property of the cementitious composites [77]. Normal tap water is adopted.

2.2 Mix proportions and fabrication of specimens

The mix proportions of the cementitious composites with different concentrations of the hybrid GNPs and CNTs are shown in Table 2. All the mixture with the same ratio of water/binders is 0.37, and the binders contain cement and fly ash. The dosage of the hybrid GNPs and CNTs is within the range of 0.0–10.0% by mass of the binders. The specimen is numbered as the concentration of the hybrid GNPs and CNTs. For example, GC1 represents the dosage of the hybrid GNPs and CNTs is 1.0 wt%. The dosage of the superplasticizer is also considered as the mass ratio of the binders.

The cementitious composites are mixed with a mixer for cement paste, as shown in Figure 2. The mix proportion with the content of the hybrid GNPs and CNTs as high as 10% by weight of binder was designed to explore the percolation threshold curve of these composites. The mix proportions with abroad ranges can offer the optimal design for piezoresistivity. Thus, such a high concentration of the GNPs and CNTs was chosen.

The water and polycarboxylate superplasticizer are added to the mixer before mixed 30 s in a beaker. Second, after dry mixing for 3 min, the fly ash and cement are added

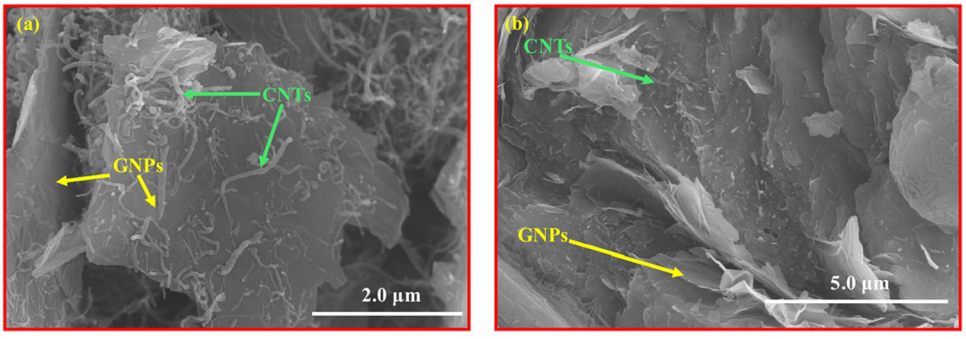

Figure 1: The typical SEM images of the hybrid GNPs and CNTs, and their dispersion in cementitious composites. (a) The typical SEM images of the hybrid GNPs and CNTs, (b) the dispersion of the hybrid GNPs and CNTs in cementitious composites.

Table 2: The numbers and mix proportions of the composites with various dosages of the hybrid GNPs and CNTs

Numbers	GNPs and CNTs (wt%)	Cement (g)	Water (g)	Superplasticizer (wt%)	Fly ash (g)
GC0	0.0	118.75	52.60	0.5	23.71
GC1	1.0	118.54	52.60	0.5	23.71
GC2	2.0	118.54	52.60	0.5	23.71
GC3	3.0	118.54	52.60	0.5	23.71
GC4	4.0	118.54	52.60	0.5	23.71
GC5	5.0	118.54	52.60	0.5	23.71
GC6	6.0	118.54	52.60	0.5	23.71
GC7	7.0	118.54	52.60	0.5	23.71
GC8	8.0	118.54	52.60	0.5	23.71
GC9	9.0	118.54	52.60	0.5	23.71
GC10	10.0	118.54	52.60	0.5	23.71

into the mixer within 60 s when it stirring using a low speed of 140 ± 5 rpm. Thereafter, the mixer is stirred for 1 min using high speed 285 ± 10 rpm. After that, the hybrid GNPs and CNTs are put into the mixer gradually for under 2 min when the mixer keeps low-speed stirring. Another 3 min mixing at high speed is conducted after all the materials have been added into the mixer. After that, the mixture is poured into molds with dimensions of 20 mm × 20 mm × 40 mm while the mixing process is finished. Two stainless steels with a distance of 20 mm and openings is 2 mm × 2 mm are used as electrodes which are embedded into the center position of each mold. Finally, the molds with the mixture are stored in a curing chamber after vibrating for 1 min with a temperature of 20 ± 3°C for 1 d. And then, the specimen is demolded and cured immersing in water at 20 ± 1°C. The dispersion of the hybrid GNPs and CNTs in cementitious composites is shown in Figure 1(b).

2.3 Test methods

Electrical resistance test is carried out after curing 28 days of the composites. The electrical resistance is tested in accordance with specification [78], and two types of measuring methods as direct current (DC) method and alternating current (AC) method are adopted to determine the resistance of specimens with digital multimeters Keithley 2100 and Agilent U1733C, respectively. Two-electrode method is employed while testing the resistance. Additionally, AC resistance is tested with different frequencies from 100 Hz to 100 kHz. Figure 3 displays resistance testing setup, which is collected by an acquisition system. Electrical resistivity ρ is obtained as equation (1) [65,79]:

$$\rho = \frac{RS}{L}, \tag{1}$$

where ρ represents electrical resistivity (Ω cm), R on behalf of electrical resistance (Ω), L is the distance between two electrodes (cm), and S stands for cross-sectional area (cm^2). Mechanical performance and piezoresistivity under compressive loading are tested by a universal electronic loading machine, and its ultimate compressive load capacity is 100 kN. Three specimens of each type of the mix proportion are measured in accordance with the specification of the American Society of Testing and Materials C109/

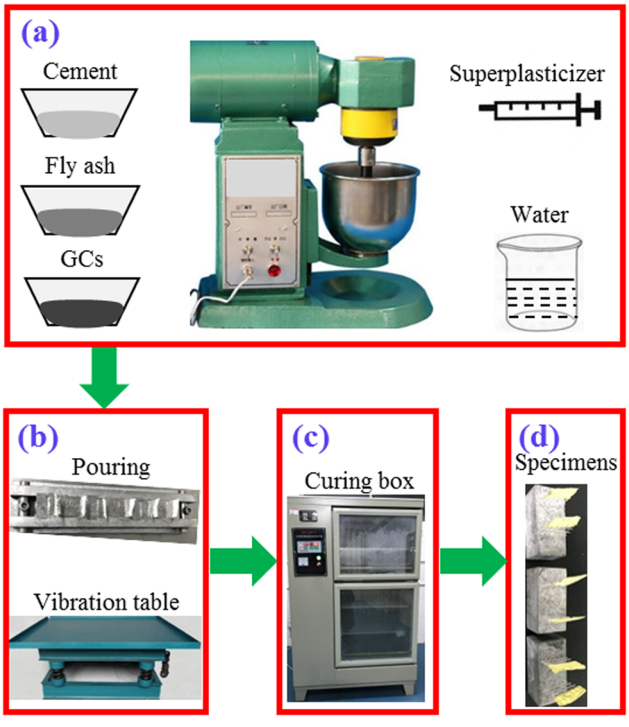

Figure 2: Diagram of specimen manufacture: (a) cement, superplasticizer, fly ash, water, and the hybrid GNPs and CNTs (GCs) and (b) poured molds and vibration table, (c) curing chamber, and (d) specimens.

C109M [80]. Strains along the longitudinal directions are measured by two strain gages with a length of 5 mm attached to the opposite surfaces of the specimen. The transverse strains on two opposite surfaces of the specimen are determined by another two strain gauges. Dynamic strain indicator DH3820N is used to collect strain. The corresponding electrical resistance is simultaneously measured by a digital multimeter (type of Keithley 2100, USA) using the DC method with two electrodes. During the testing process on resistance, load, and strain, the frequency was adopted as 2 Hz and the loading rate was 0.4 mm/min. The load, strain, and resistance are collected by an acquisition system, and Figure 4 displays the test instruments. The FCR is expressed as equation (2) [79]:

$$\mathrm{FCR} = \frac{\rho - \rho_0}{\rho_0} \times 100\%, \tag{2}$$

where ρ_0 represents initial electrical resistivity and ρ stands for electrical resistivity subjects to the max load.

3 Results and analysis

3.1 Mechanical performances

Figure 5 shows the mechanical performances of GC0–GC10 to withstand compressive load from loading to failure. Figure 5(a) displays a comparison of relationships between stress and strain of cementitious composites containing the hybrid GNPs and CNTs with different contents. It can be seen from Figure 5(a) that the stress–strain curves of GC0–GC10 present brittleness characteristics and the stress almost linear growth with the strain until the maximum stress. In addition, the maximum stress of GC1–GC3 is higher than that of GC0, but GC4–GC10 is lower than that of GC0 while the dosage of hybrid GNPs and CNTs varied within the ranges of 0.0–10.0 wt%. Meanwhile, the maximum stress is decreased upon increasing dosage from 2.0 to 10.0 wt% of hybrid GNPs and CNTs. Figure 5(c) displays the ultimate strain corresponding to the maximum stress of GC0–GC10; they ranged from 3,990 to 5,660 με. The slope of the stress–strain curves of GC1–GC3 is higher than that of GC0, but GC4–GC10 is lower than that of GC0. Meanwhile, the slope is decreased with increasing dosage from 2.0 to 10.0 wt% of hybrid GNPs and CNTs.

The maximum stress stands for compressive strength, as displayed in Figure 5(b) that the compressive strength of GC0–GC10 is 82.5, 93.0, 108.1, 90.0, 78.5, 73.3, 71.8, 66.0, 64.1, 61.0, and 46.6 MPa, respectively. The compressive strength of GC1–GC3 is correspondingly increased by 12.8, 31.1, and 9.2% compared with GC0. It means that the dosage of the hybrid GNPs and CNTs no more than 3.0 wt% can disperse homogenously and generate microfiber as well as hydration nucleation effect synergistic in cementitious composites [81,82], as shown in Figure 6. It demonstrates generating, initiating, and developing of cracks can be decreased and restrained by the microfiber effect of the hybrid GNPs and CNTs. Thus presents a positive synergetic enhancing effect on strength when the dosage is no more than 3.0 wt%. On the contrary, the compressive strength of GC4–GC10 is decreased by 4.8, 11.1, 12.9, 20.0, 22.2, 26.1, and 43.5%, respectively. However, the compressive strength of GC4–GC10 can still be achieved from 46.6 to 78.5 MPa. This is caused by

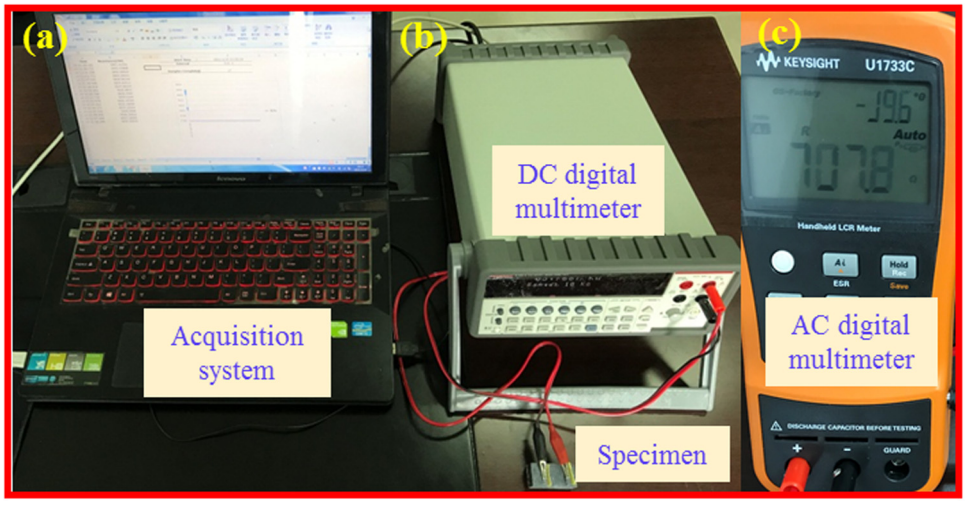

Figure 3: The resistance testing setup: (a) Acquisition system, (b) DC digital multimeter, and (c) AC digital multimeter.

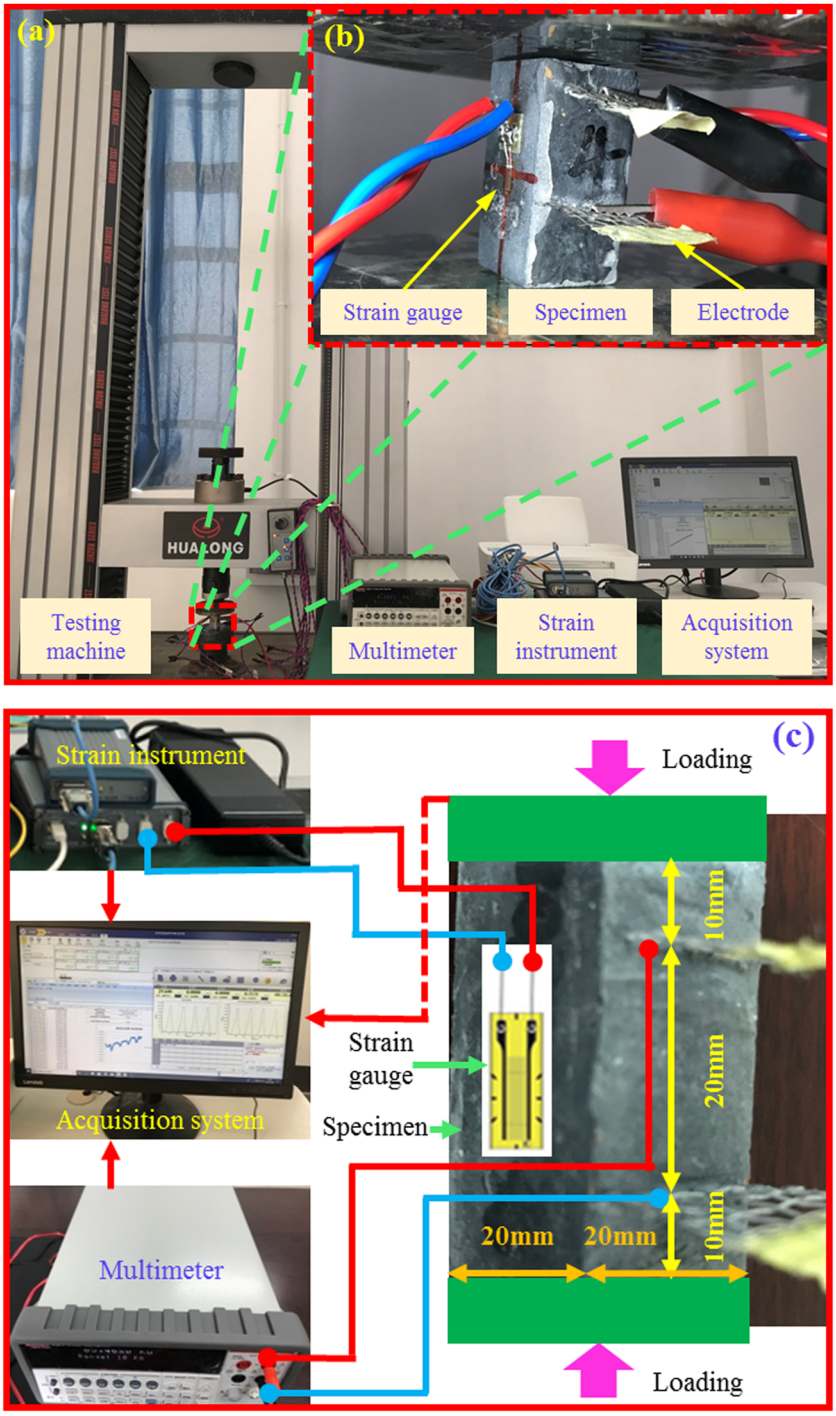

Figure 4: Experimental configuration of piezoresistivity testing setup: (a) Photograph of overall piezoresistivity testing setup, (b) local magnification of piezoresistivity testing setup, and (c) schematic of piezoresistivity testing setup.

aggregations and strong absorbency of the hybrid GNPs and CNTs. When the dosage is no more than 3.0 wt%, they are dispersed homogenously in cementitious composites, as shown in Figure 6(b). While the dosage is more than 3.0 wt%, aggregations in cementitious composites are more likely to occur for huge specific surface areas and strong Van der Waals force [83], which is displayed in Figure 6(c) and (d). In addition, with increasing dosage of the hybrid GNPs and CNTs, the workability of the cementitious composites becomes worse because of their strong water absorption [84,85]. In addition, the air bubbles and defects are increased in the cementitious composites. Therefore, with

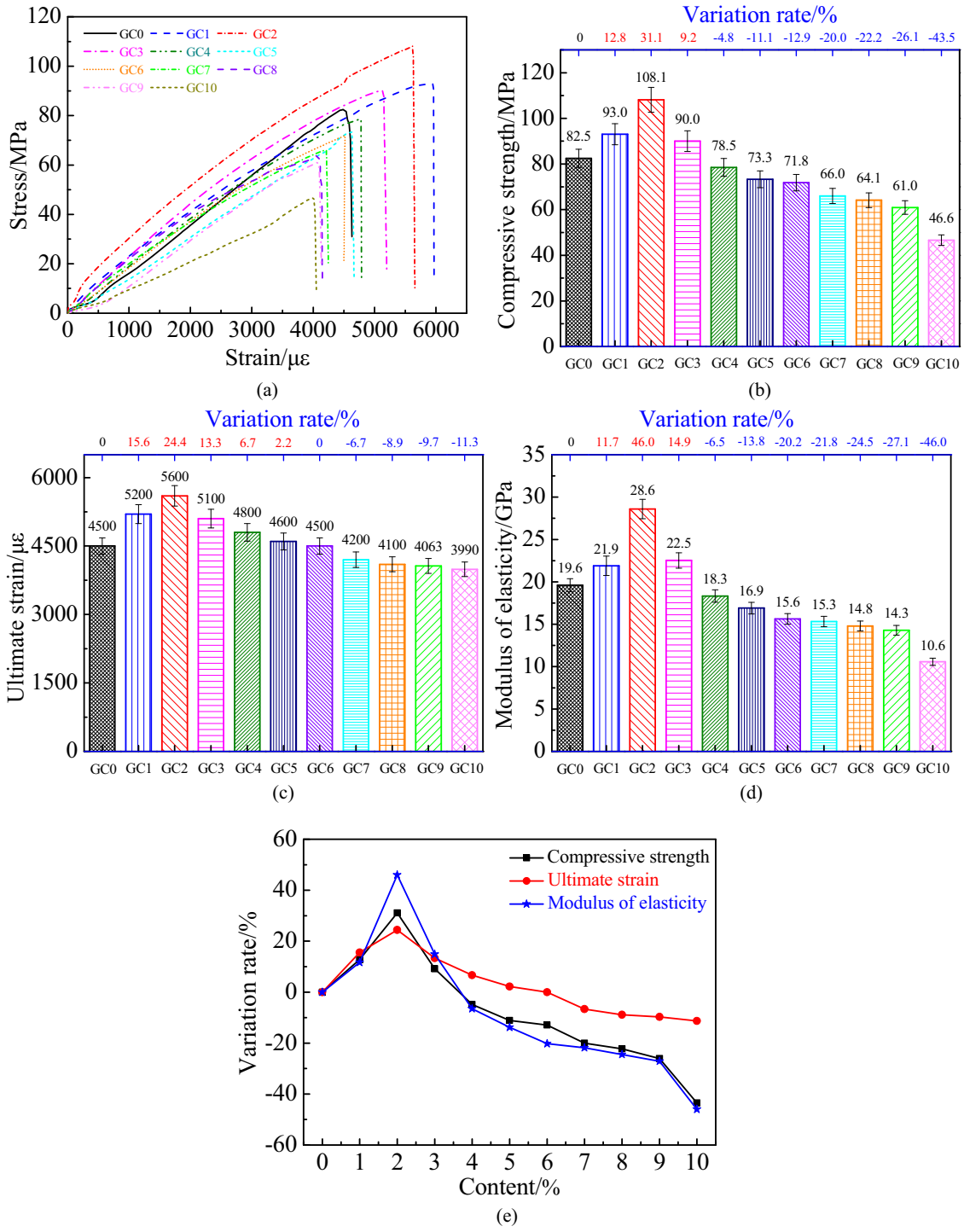

Figure 5: Mechanical properties of GC0–GC10 subject to monotonic compressive load. (a) Stress–strain curves, (b) compressive strength, (c) ultimate strain, (d) modulus of elasticity, and (e) variation rate of mechanical properties.

the increase of the hybrid GNPs and CNTs from 4.0 to 10.0 wt%, the strength decreased gradually.

It also can be obviously observed from Figure 5(e) that the variable tendency of the strength increased first until the dosage of the hybrid GNPs and CNTs is 2.0 wt% and then decreased with the concentration growths under scope of 3.0–10.0 wt%. As shown in Figure 5(b), (c), and (e), the variation tendency of the ultimate strain resembles as that of the strength. However, only the ultimate strain of GC7–GC10 is decreased compared with GC0, while the

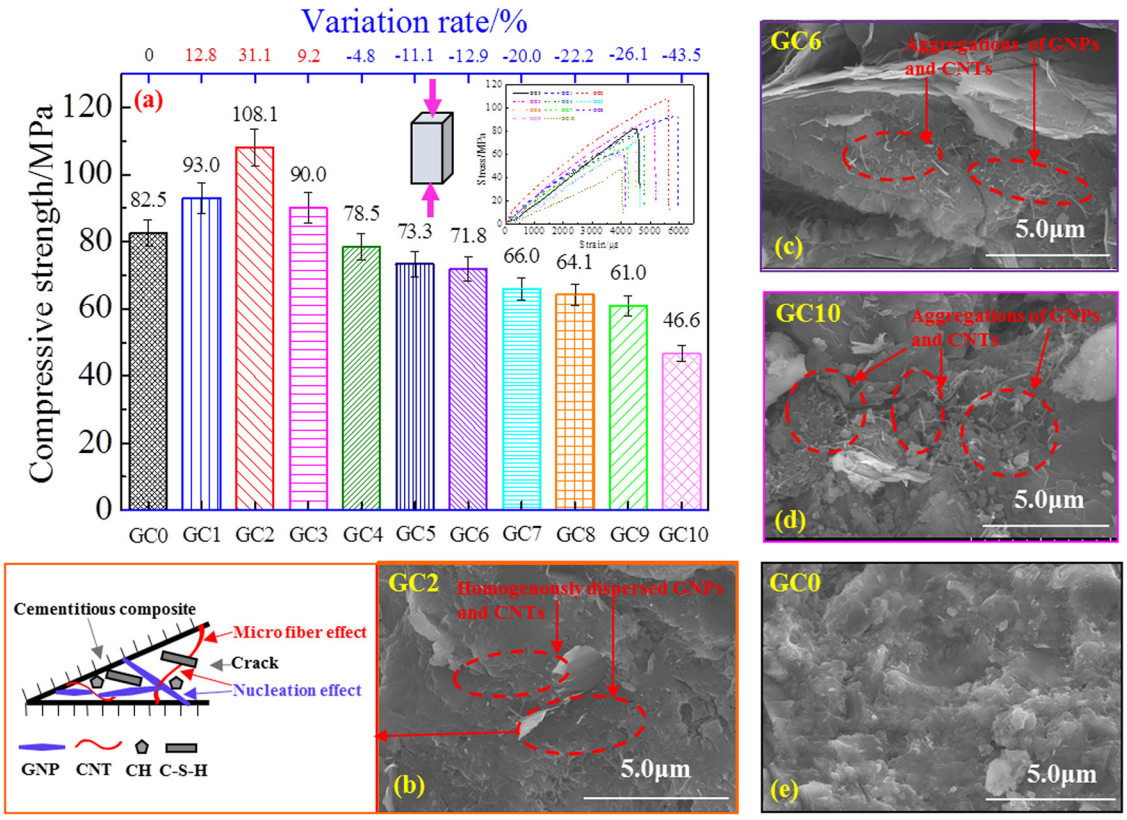

Figure 6: Modification mechanisms on mechanical properties and the hybrid GNPs and CNTs disperse in cementitious composites, (a) compressive strength, (b) GC2, (c) GC6, (d) GC10, and (e) GC0.

strength of GC4–GC10 is decreased compared with GC0. The increase and decrease rates of the ultimate strain are within the ranges of 2.2–24.4% and 0.0–11.3%, respectively. Additionally, GC2 and GC10 present the highest and the lowest ultimate strains of 5,600 and 3,990 με, respectively. They are correspondingly increased and decreased 24.4 and 11.3%, respectively. The ultimate strain reflects the deformation capacity of the composites. This implies that the development of cracks can be efficient restraint and the ductility can be enhanced by the hybrid GNPs and CNTs with content no more than 6.0 wt% with effect includes bridging and pulled-out/off, as shown in Figure 6(b). Meanwhile, the hybrid GNPs and CNTs can also correspondingly restrain the lateral deformation and increase deformation along the longitudinal direction, respectively. This phenomenon is also demonstrated by Dong [3].

The modulus of elasticity can be computed according to the relationships between stress and strain under the elastic regime, which is often set as 40% of the maximum stress. Stress is changed proportionally with strain during this stage in accordance with the specifications [86]. Figure 5(d) indicates the modulus of elasticity corresponding to GC0–GC10 is 19.6, 21.9, 28.6, 22.5, 18.3, 16.9, 15.6, 15.3, 14.8, 14.3, and 10.6 GPa, respectively. The modulus of elasticity is comparable to the result of references [3,29]. As presented in Figure 5(b), (d), and (e), the variation tendency of the modulus of elasticity is also similar to that of the compressive strength. The modulus of elasticity corresponding to GC1–GC3 is raised by 11.7, 46.0, and 14.9%, respectively. However, the decreasing scope of the modulus of elasticity of GC4–GC10 is from 6.5 to 46.0%.

The typical failure modes of the composites are shown in Figure 7. As shown in Figure 7, the fragments at the failure state are raised upon increasing the hybrid GNPs and CNTs. This also demonstrates that cementitious composites exhibit good ductility. As mentioned earlier, the hybrid GNPs and CNTs can disperse homogenously in cementitious composites with a content of no more than 3.0 wt%, and contribute as microfiber and hydration nucleation effect synergistic. Therefore, original cracks are reduced, and development of existing cracks is inhibited and mechanical properties are improved. However, the defects increase when the dosage of the hybrid GNPs and CNTs more than 3.0 wt% for their high specific surface areas, huge van der Waals force, and water absorption, which is harmful for the mechanical properties.

3.2 Electrical properties

The electrical resistivity of the composites tested by the DC method is shown in Figure 8. As shown in Figure 8(a)–(c), the DC electrical resistivity reduces from 141,120 to 78 Ω cm when the dosage of the hybrid GNPs and CNTs grows from 0.0 to 10.0 wt%. The electrical resistivity of GC8, GC9, and GC10 is 2,420, 630, and 78 Ω cm, respectively. Therefore, the electrical resistivity measured using the DC method is decreased by up to three orders due to the synergistic improving effect of the hybrid GNPs and CNTs on electrical conductivity. The electrical resistivity of GC10 measured by the DC method is one order of magnitude lower than the cementitious composites containing 10.0 wt% GNPs [87], it also indicates the hybrid GNPs and CNTs present a cooperation-enhancing effect on electrical conductivity is better than that of the single GNPs. Additionally, the DC electrical resistivity of GC10 is lower than the electrical resistivity of cementitious composite incorporating 1.0 vol% CNTs [88].

Electrical resistivity measured by the DC method decreases slightly when the dosage of the hybrid GNPs and CNTs less than 1.0 wt% and within the scope of 6.0–10.0 wt%. However, as the dosage of the hybrid GNPs and CNTs increases from 1.0 to 6.0 wt %, it decreases dramatically and reaches up to three orders. Therefore, the percolation threshold zone of these composites is within the scope of 1.0–6.0 wt%.

Mechanisms of the hybrid GNPs' and CNTs' influence on electrical conduction is shown in Figure 9. The average separation among the hybrid GNPs and CNTs is long when the dosage is lower than 1.0 wt%. Therefore, the electrical resistivity is greatly influenced by the cement hydration degree due to the electrical conduction method mainly relying on a small amount of electrons and electrolyte ions transfer, which can be shown in Figure 9(a). Subsequently, the electrically conductive networks are formed gradually with increasing concentrations of 1.0–5.0 wt%. The electrically conductive way of the cementitious composites is changed from main relays on both electrolyte ions and a small number of electrons transferred to mainly depending on electrons transfer, which is shown in Figure 9(b). The stable electrically conductive networks are formed within cementitious composites when the dosage increases

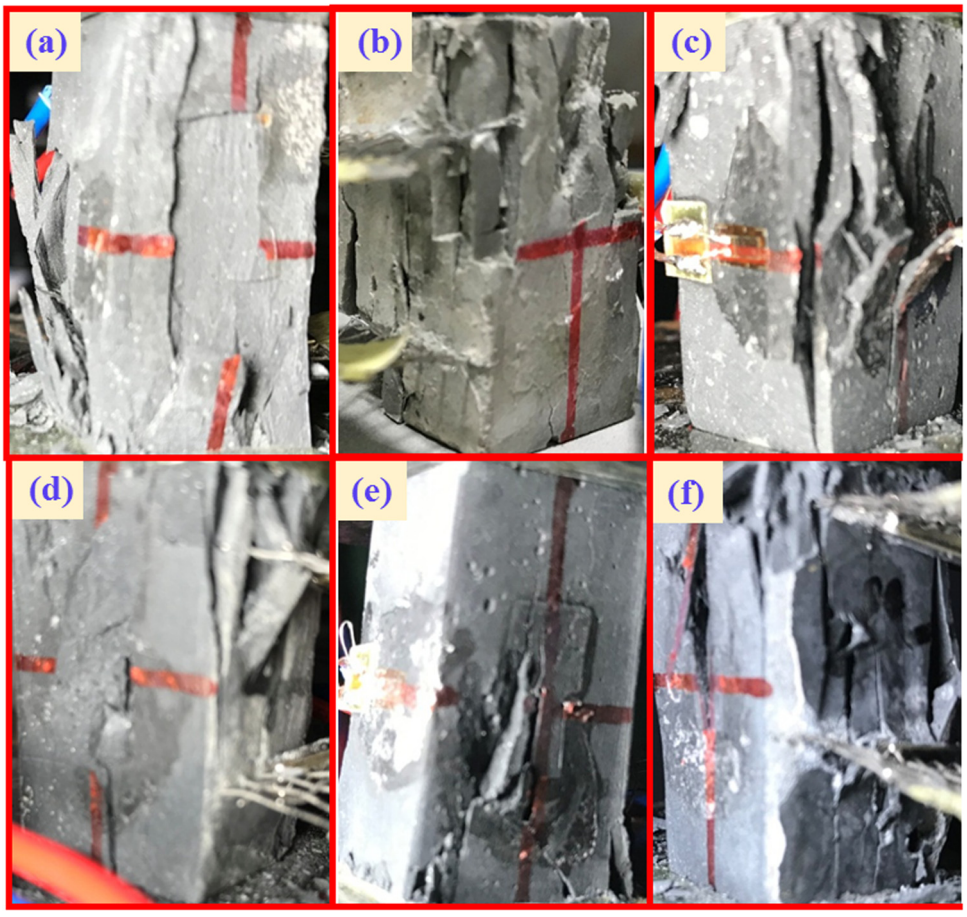

Figure 7: Failure modes of the specimens: (a) GC0, (b) GC2, (c) GC4 (d) GC6, (e) GC8, and (f) GC10.

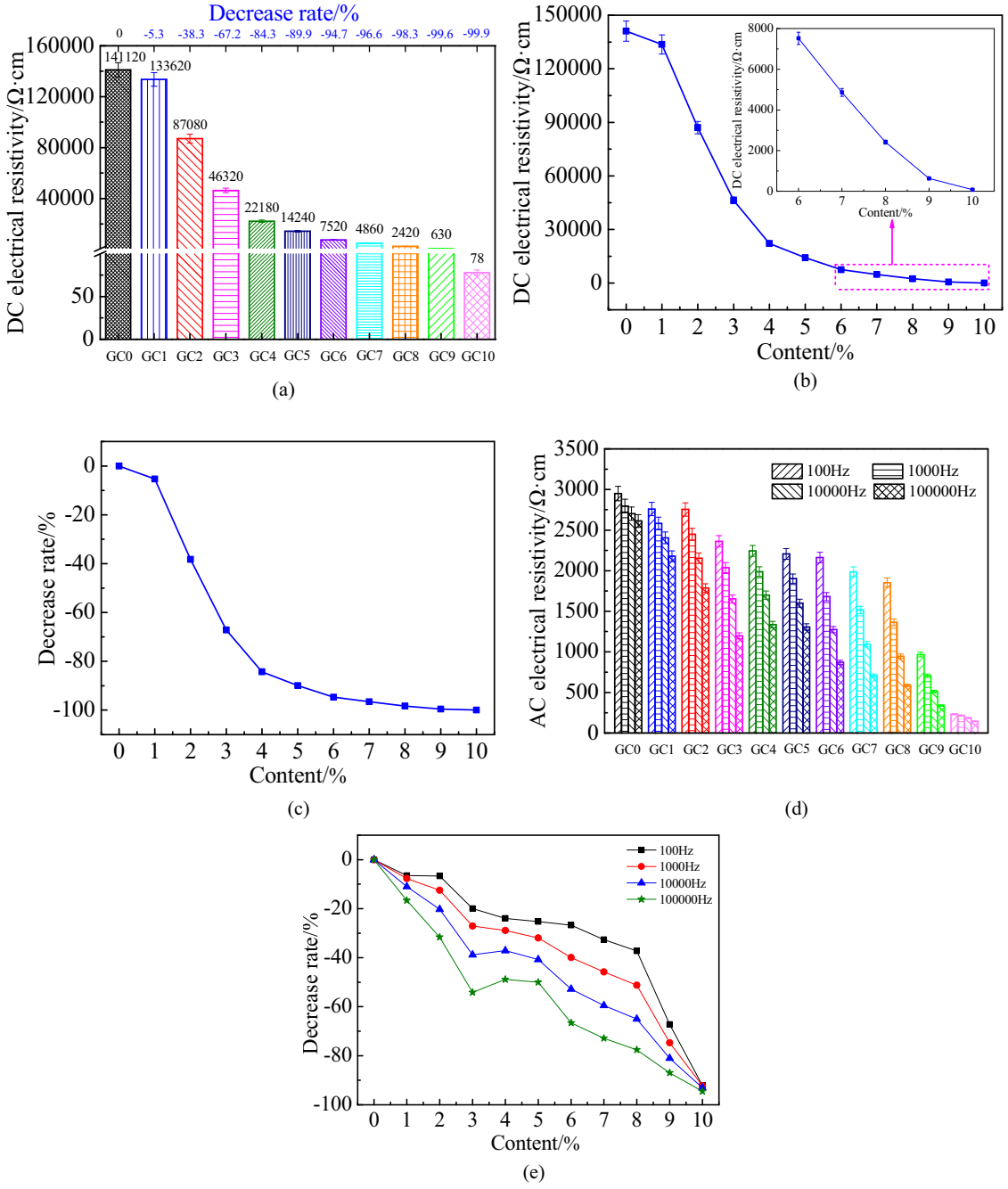

Figure 8: Electrical properties of GC0–GC10. (a) DC electrical resistivity, (b) percolation threshold of DC electrical resistivity, (c) decrease rate of DC electrical resistivity, (d) AC electrical resistivity, (e) decrease rate of AC electrical resistivity.

to the ranges of 6.0–8.0 wt%. The electrical conduction of the cementitious composites mainly relies on the tunnel effect caused by electrons, as shown in Figure 9(c). Some GNPs and CNTs overlap with the dosage continuously increasing to the ranges of 9.0–10.0 wt%. Thus, the electrical conduction mainly depends on contact conduction, which is shown in Figure 9(d).

Mechanisms of synergistic enhancing influence of the hybrid GNPs and CNTs on the electrical conductivity are illustrated in Figure 10. Both the GNPs and CNTs possess a big specific surface area and outstanding electrical conductivity. Additionally, the nanostructures of the GNPs and CNTs are corresponding to two-dimensional platelets and one-dimensional tubes, respectively. The high aspect ratio

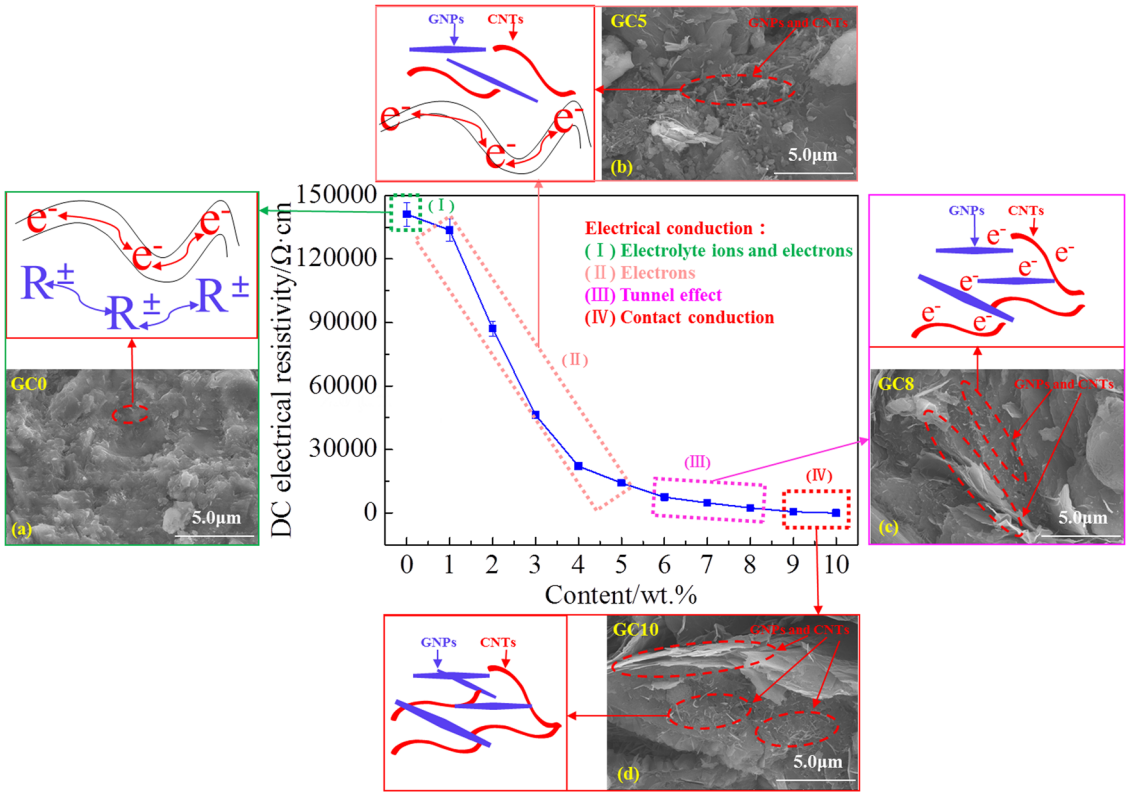

Figure 9: Mechanisms of hybrid GNPs and CNTs on electrical conductivity of the composites: (a) GC0, (b) GC5, (c) GC8, and (d) GC10.

and different dimensions, sizes, and shapes in nanoscale are convenient to produce electrically conductive pathways and networks within cementitious composites by cooperation enhancing effect.

Figure 8(d) and (e) display the electrical resistivity of the composites measured by the AC method. The AC electrical resistivity decreased upon increasing the dosage of the hybrid GNPs and CNTs at different frequencies. The AC electrical resistivity of GC0–GC10 varies from 2,950 to 232 Ω cm at a frequency of 1.0×10^2 Hz. In addition, the electrical resistivity of GC0–GC10 decreases upon increasing frequency from 1.0×10^2 to 1.0×10^5 Hz because high frequency can weaken the polarization effect [2]. Compared with GC0, the decrease rates of GC1–GC10 at frequencies of 1.0×10^2, 1.0×10^3, 1.0×10^4 and 1.0×10^5 Hz are within the ranges of 6.4–92.1%, 7.7–92.3%, 11.0–93.1%, and 16.6–94.5%, respectively.

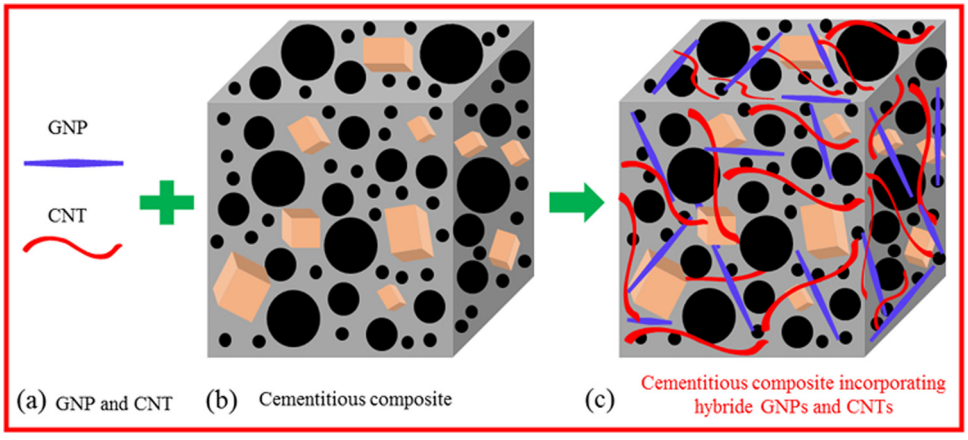

Figure 10: Mechanisms of synergistic enhancing effect of the hybrid GNPs and CNTs influence on electrical conductivity: (a) microstructures of the GNPs and CNTs, (b) microstructures of cementitious composites, and (c) microstructures.

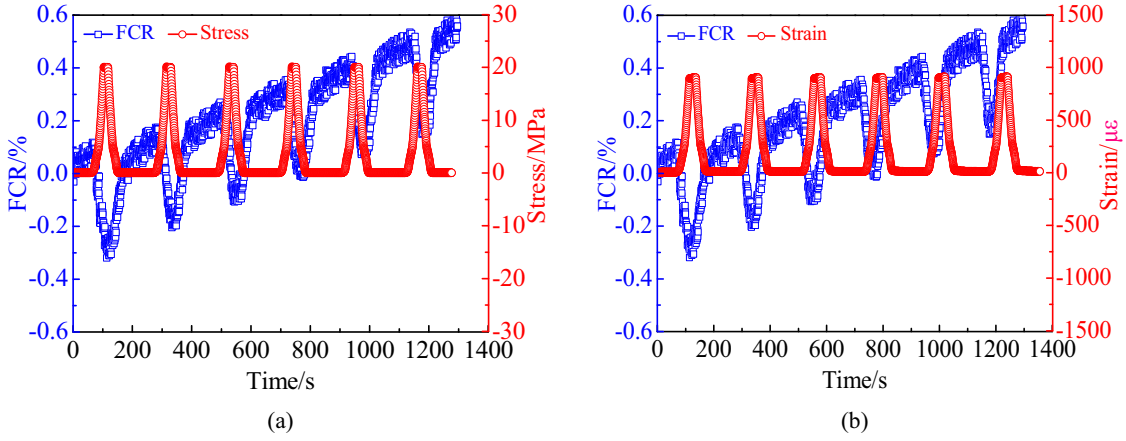

Figure 11: Relationships between FCR and repeated stress/strain of GC0. (a) FCR–stress curves, and (b) FCR–strain curves.

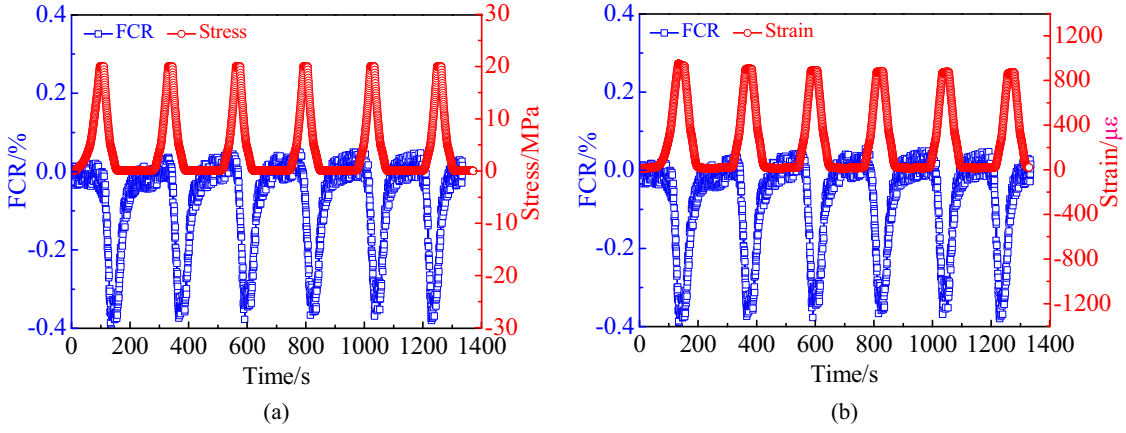

Figure 12: Relationships between FCR and repeated stress/strain of GC1.

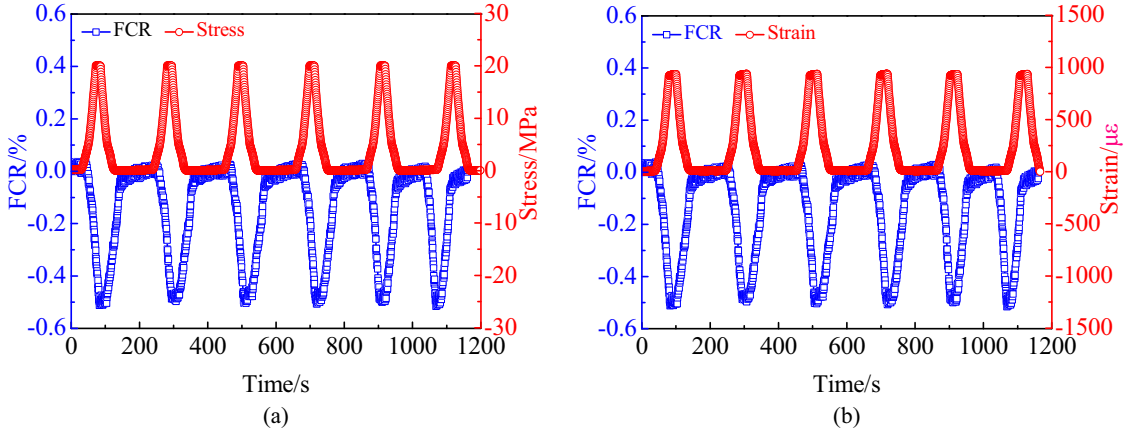

Figure 13: Relationships between FCR and repeated stress/strain of GC2. (a) FCR–stress curves, and (b) FCR–strain curves.

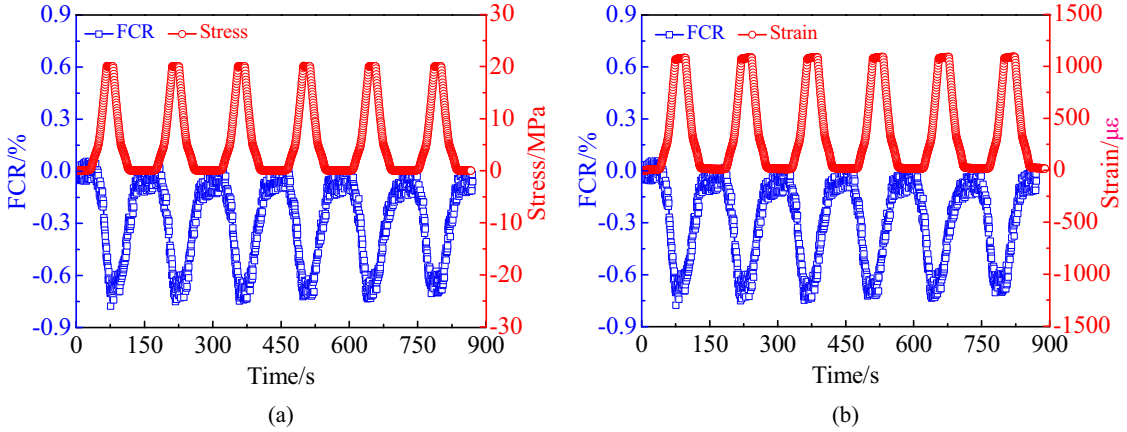

Figure 14: Relationships between FCR and repeated stress/strain of GC3. (a) FCR–stress curves, and (b) FCR–strain curves.

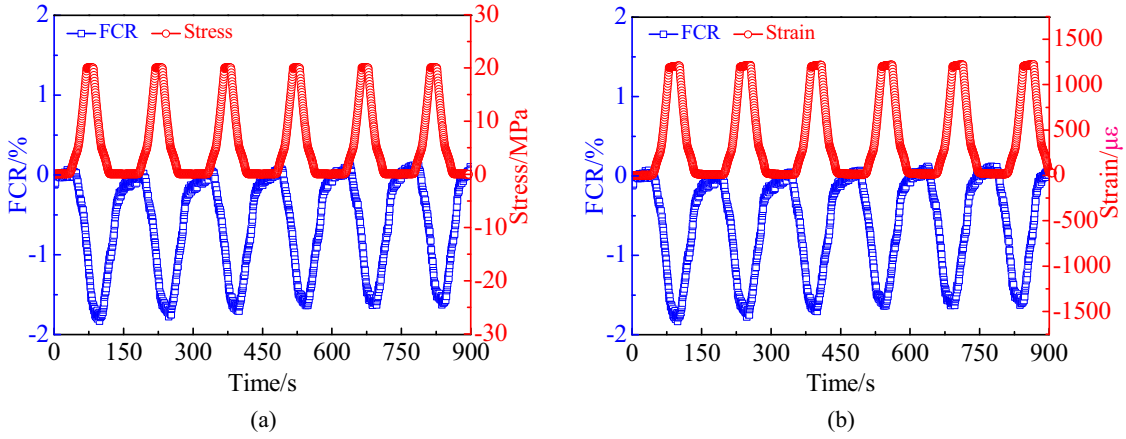

Figure 15: Relationships between FCR and repeated stress/strain of GC4. (a) FCR–stress curves, and (b) FCR–strain curves.

The electrical resistivity of GC10 is 232 Ω cm, which is decreased by one order compared with GC0 at a frequency of 1.0×10^2 Hz.

As shown in Figures 9 and 10, the hybrid GNPs and CNTs possessing big aspect ratios and different dimensions, sizes, and shapes in the nanoscale are convenient for

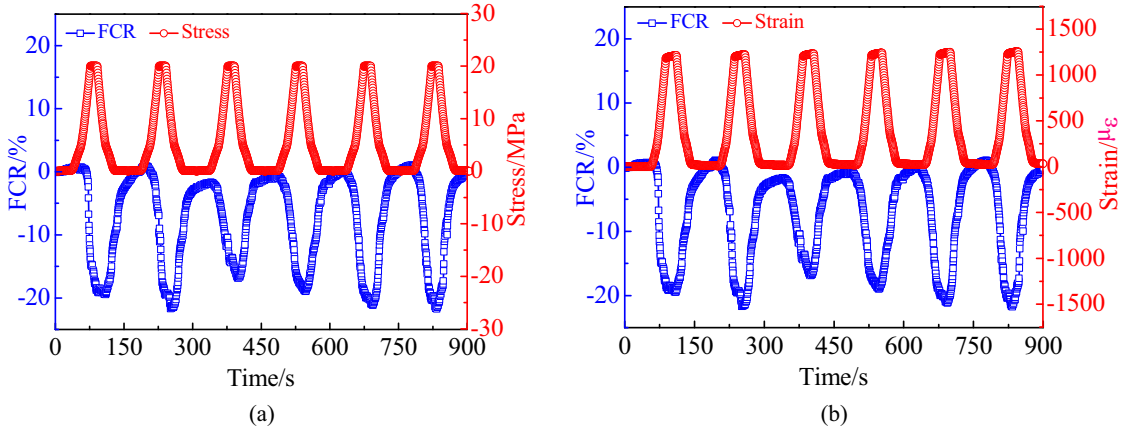

Figure 16: Relationships between FCR and repeated stress/strain of GC5. (a) FCR–stress curves, and (b) FCR–strain curves.

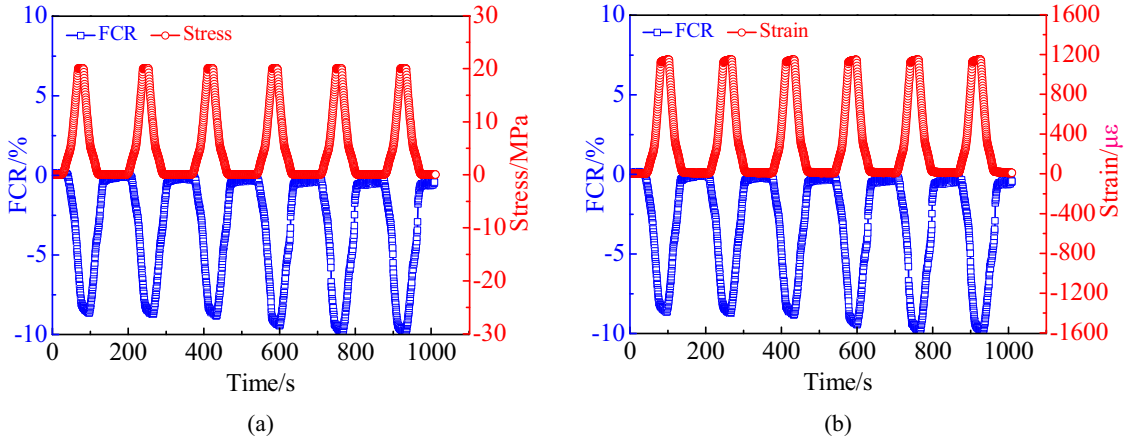

Figure 17: Relationships between FCR and repeated stress/strain of GC6. (a) FCR–stress curves, and (b) FCR–strain curves.

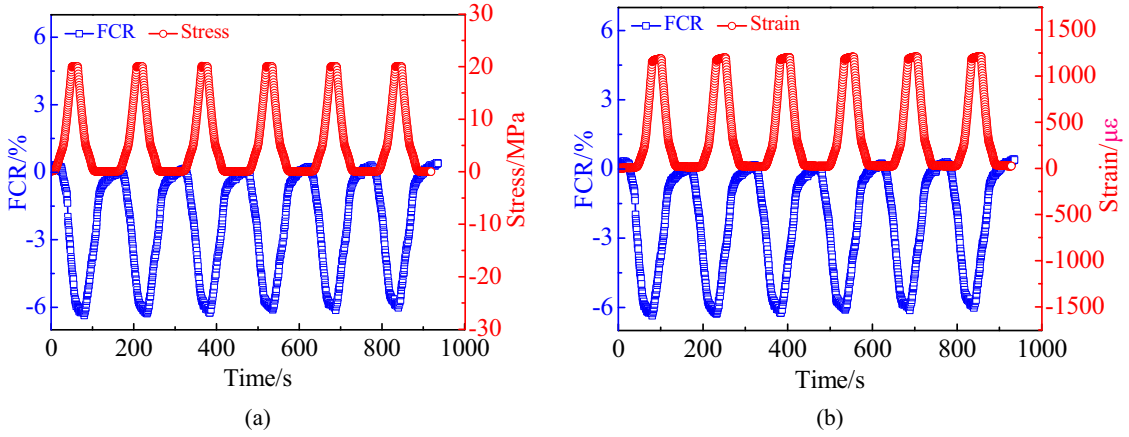

Figure 18: Relationships between FCR and repeated stress/strain of GC7. (a) FCR–stress curves, and (b) FCR–strain curves.

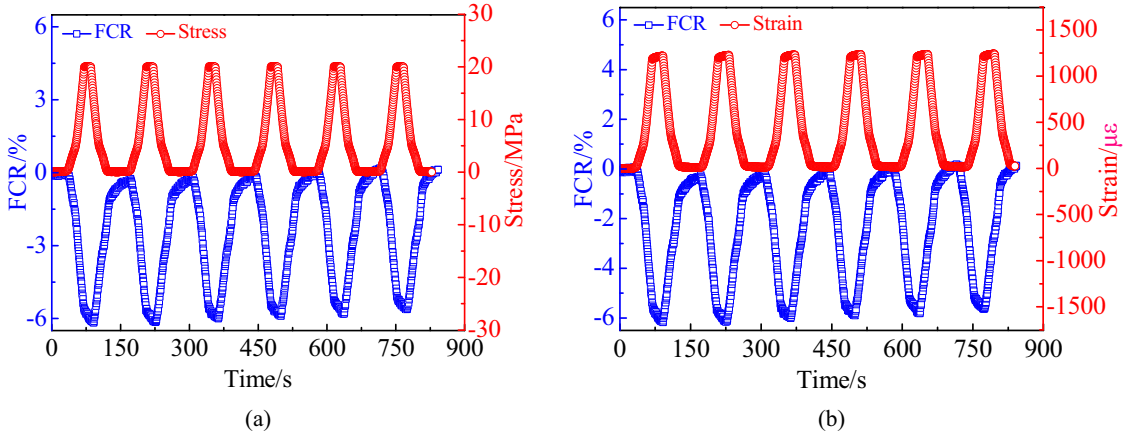

Figure 19: Relationships between FCR and repeated stress/strain of GC8. (a) FCR–stress curves, and (b) FCR–strain curves.

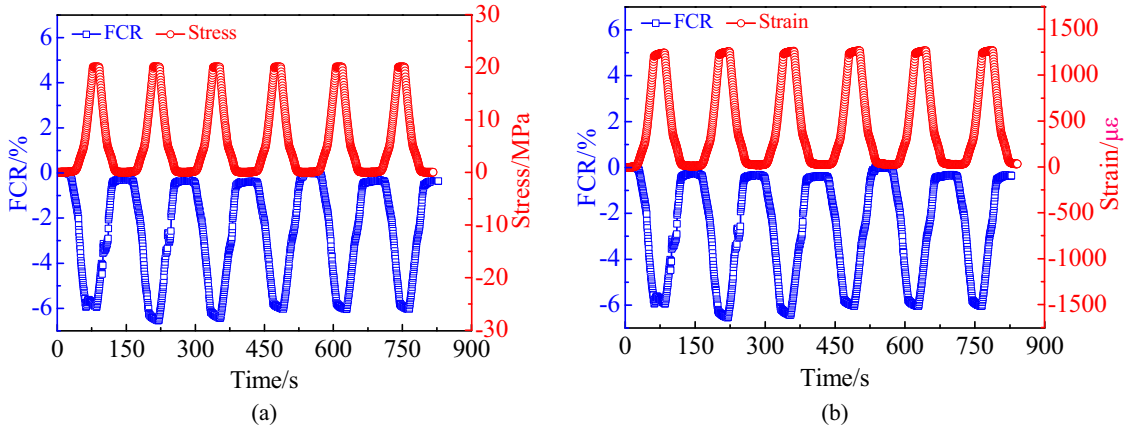

Figure 20: Relationships between FCR and repeated stress/strain of GC9. (a) FCR–stress curves, and (b) FCR–strain curves.

generating electrically conductive networks with synergistic enhancing effect. Therefore, the percolation threshold of the composites can be realized by lower content.

3.3 Piezoresistivity

3.3.1 Piezoresistivitive performances withstand repeated compression

Relationships between FCR and stress/strain of GC0–GC10 after curing 28d subject to repeated compression with stress of 20 MPa are displayed in Figures 11–21. As demonstrated in Section 3.2, the percolation threshold zone of these composites is within the scope of 1.0–6.0 wt%. Therefore, the piezoresistitive performances withstand repeated compression separated into three parts before percolation, during percolation, and after percolation. The relationships between the FCR and stress/strain of the cementitious composite with the concentration of 5.0 wt% of the GNPs and CNTs which is during percolation are as follows. The FCR reduces with the stress/strain increases, and it returns to the beginning state with the stress/strain reduced, which is shown in Figure 16. Additionally, the variety rules of FCR with stress/strain of GC0–GC10 are almost the same as each other. However, the electrical resistivity of GC0 is slightly increased with time because of the polarization effect (as shown in Figure 11), while the piezoresistive performances of GC1–GC10 present good repeatability and stability (as shown in Figures 12 to 21). With the dosage of the hybrid GNPs and CNTs increasing, signal-to-noise ratio is raised.

The maximum absolute value of FCR and stress/strain sensitivity under repeated compression of GC0–GC10 is displayed in Figure 22. As shown in Figure 22, both the maximum absolute FCR and stress/strain sensitivities of GC0–GC10 firstly increase then decrease and almost keep constant at last with dosage increases from 0.0 to 10.0 wt%. Figure 22 indicates that the maximum absolute value of

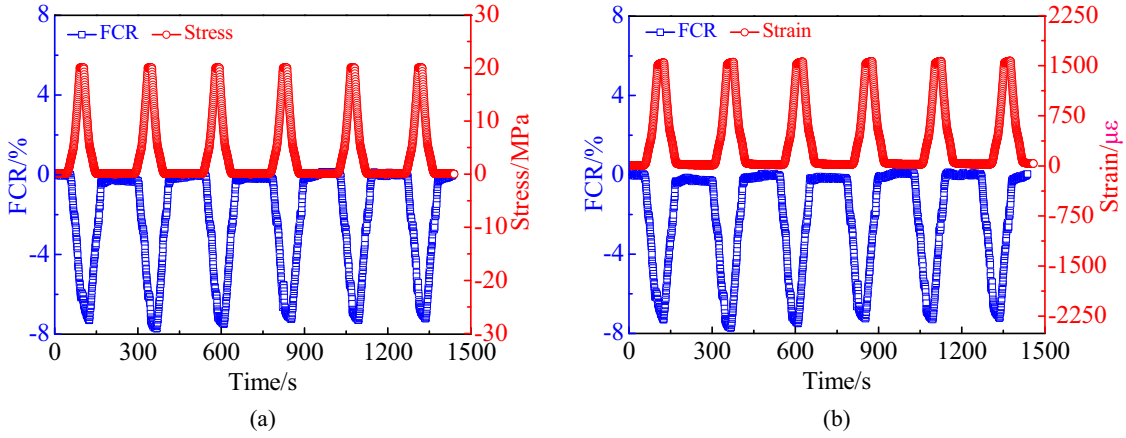

Figure 21: Relationships between FCR and repeated stress/strain of GC10. (a) FCR–stress curves, and (b) FCR–strain curves.

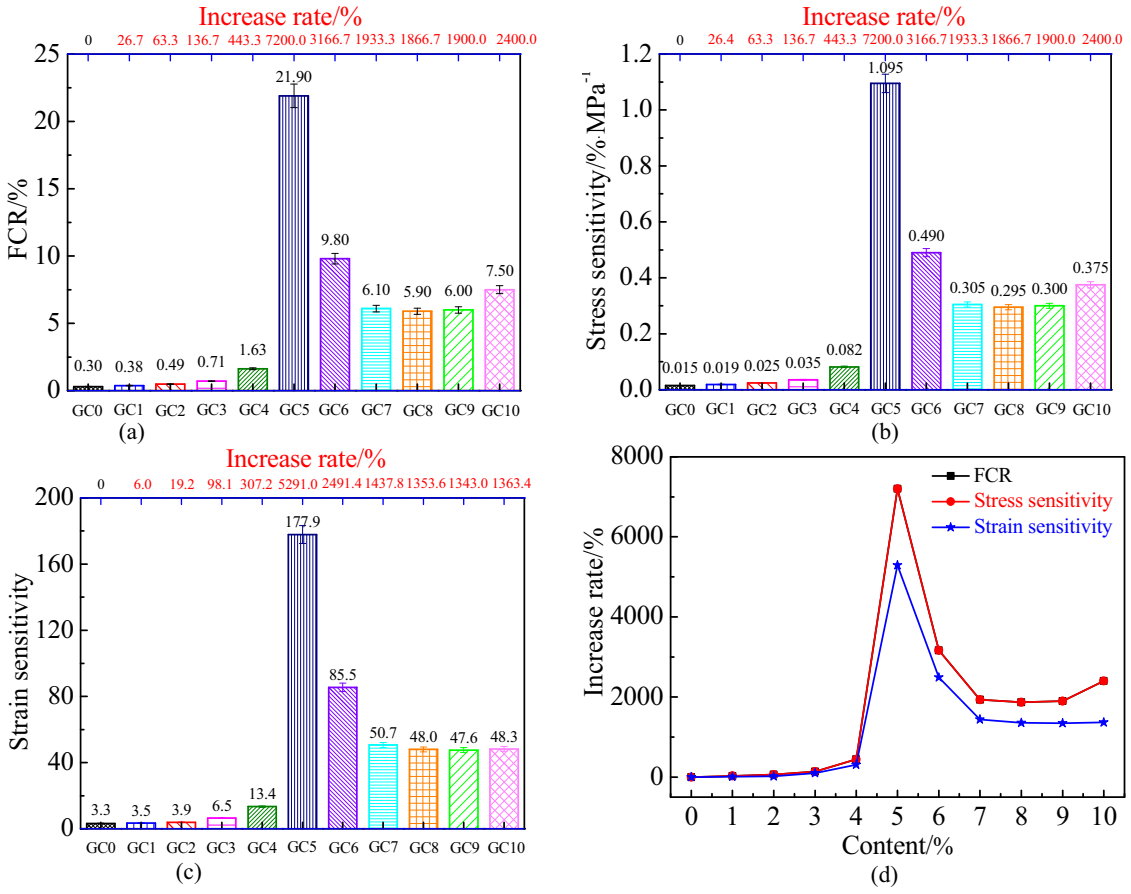

Figure 22: The maximum absolute FCR and sensitivities under repeated compression. (a) The maximum absolute FCR, (b) stress sensitivity, (c) strain sensitivity, and (d) increase rate of the maximum absolute FCR and sensitivities.

FCR and sensitivities are within ranges of 0.30–21.9%, 0.015–1.1% MPa^{-1}/3.3–177.9, respectively. Compared with GC0, the increase rate of the maximum absolute value of FCR and sensitivities of GC1–GC10 is within the ranges of 26.7–7,200.0% and 26.4–7,200.0%/6.0–5,291.0%, respectively. The stress/strain sensitivities and the maximum absolute FCR show similar variation tendencies. Therefore, the mechanisms of these phenomena are also similar to each other. GC5 displays the best piezoresistive performance and its maximum absolute FCR and stress/strain sensitivities can be achieved at 21.90 and 1.1% MPa^{-1}/177.9, respectively.

When the contents of the hybrid GNPs and CNTs are lower than 5.0 wt% and within the scope of 6.0–10.0 wt%, the maximum absolute FCR is less than 1.63% and in the ranges of 5.90–9.80%, respectively. The maximum absolute FCR reaches up to 21.9% with a dosage of 5.0 wt%. When the dosage is lower than 5.0 wt%, the distance between GNPs and CNTs is long. Thus, the conductive pathways

Table 3: Comparison of the piezoresistivity of the cementitious composites under repeated compression

Functional fillers	Content	FCR	Stress sensitivity/% MPa^{-1}	Strain sensitivity	Ref.
GNPs and CNTs	5.0 wt%	21.9	1.095	177.9	This article
GNPs	9.0 wt%	—	—	16.7	[3]
GNPs	5.0 vol%	—	0.780	—	[91]
CNTs	0.5 vol%	—	0.4000	54.0	[77]
Carbon black and pp fibers	0.5 + 0.5 wt%	—	0.69–1.06	—	[72]
Carbon black	2.0 wt%	17.5	—	—	[92]

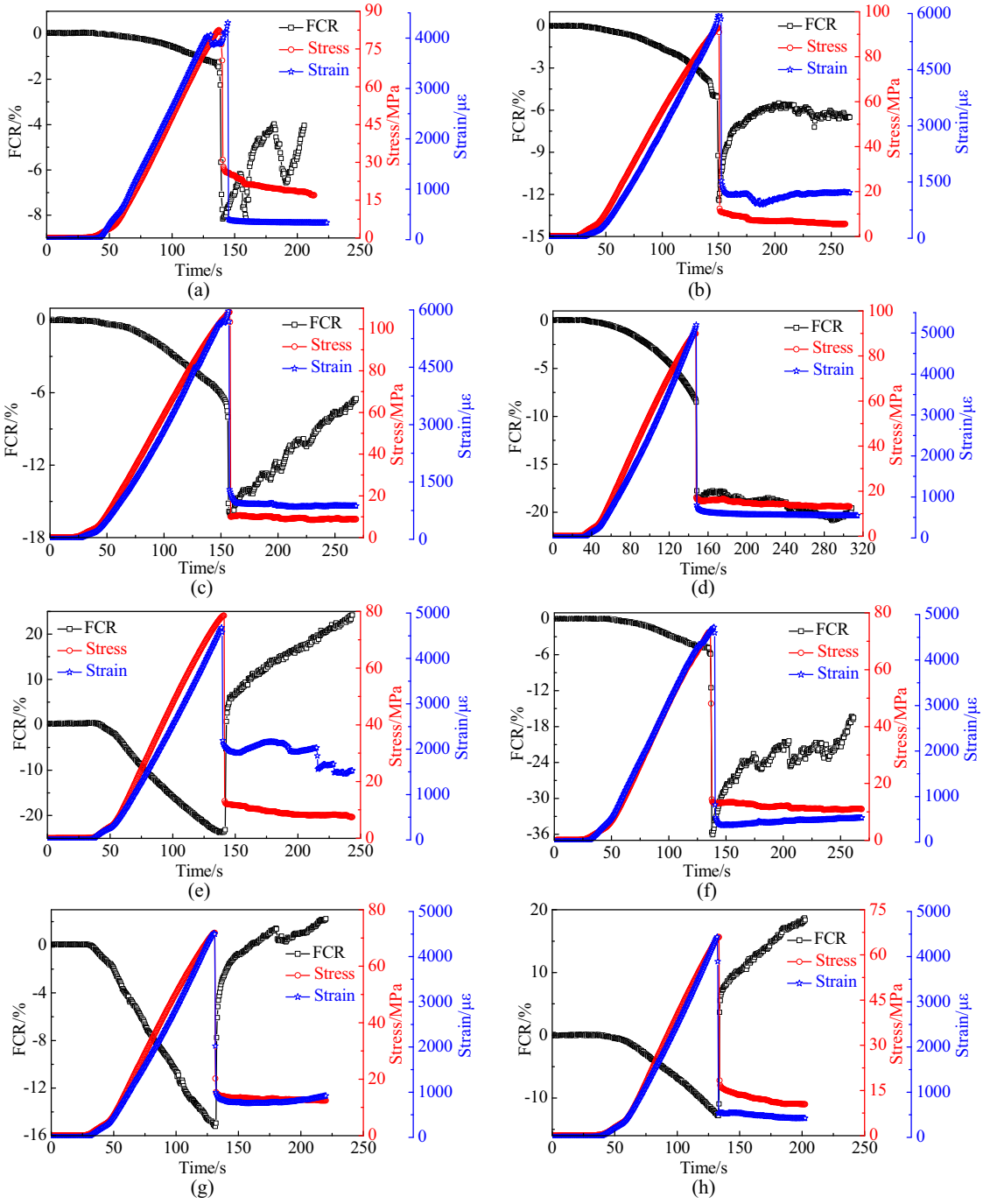

Figure 23: Relationships of FCR and stress/strain withstand monotonic compression. (a) GC0, (b) GC1, (c) GC2, (d) GC3, (e) GC4, (f) GC5, (g) GC6, (h) GC7, (i) GC8, (j) GC9, (k) GC10.

increasing with the compressive stress/strain are less. However, there are a lot of conductive pathways exist even without compression when the dosage is increased to more than 5.0 wt%. Therefore, the maximum absolute value of FCR and sensitivities first increases, then decreases, and almost keeps constant at last when increasing the dosage of the hybrid GNPs and CNTs. It is also observed by Han and coauthors [89,90].

Table 3 gives the comparison of the piezoresistivity of the cementitious composites under repeated compression. It shows that the stress/strain sensitivities in the present article are the highest comparison on cementitious

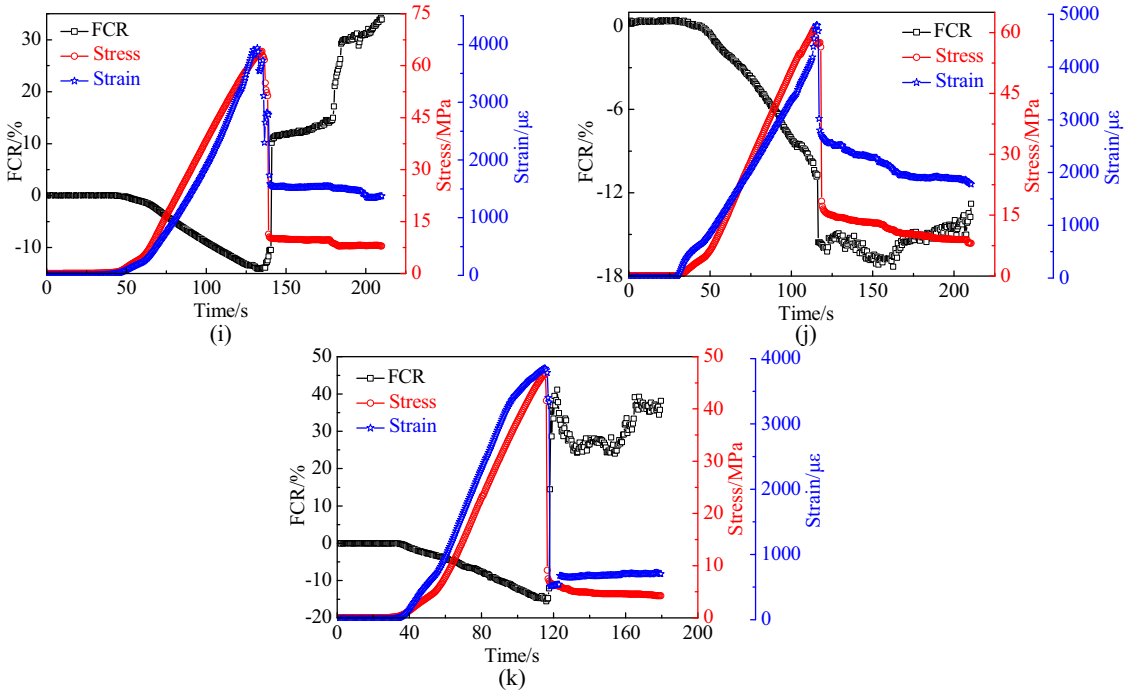

Figure 23: (*Continued*)

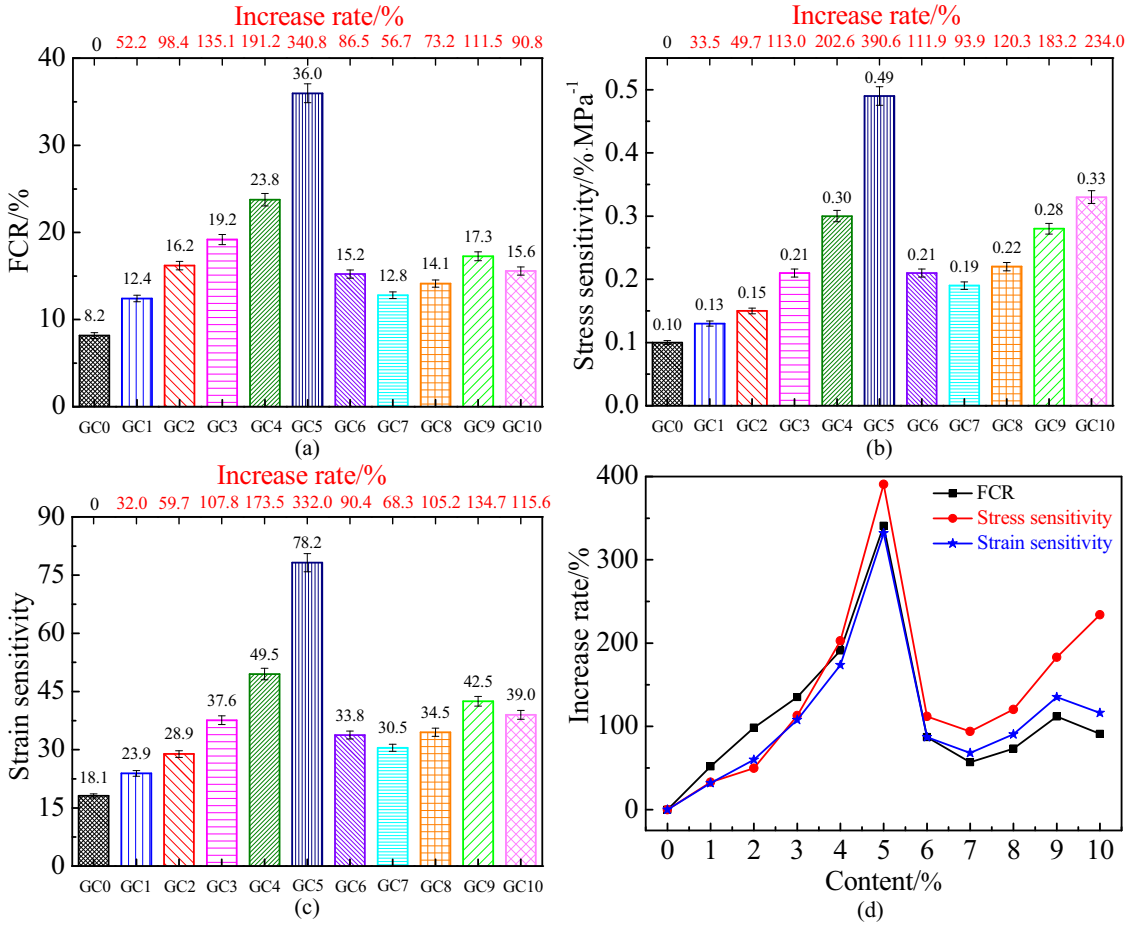

Figure 24: FCR and sensitivities under monotonic load. (a) Absolute value of FCR, (b) stress sensitivity, (c) strain sensitivity, and (d) increase rate of FCR and sensitivities.

Table 4: Comparison of the sensitivities of the composites including nanocarbon functional fillers under monotonic load

Functional fillers	Content	FCR	Stress sensitivity/% MPa^{-1}	Strain sensitivity	Ref.
GNPs and CNTs	5.0 wt%	36.0	0.49	78.2	This article
CNTs and CFs	0.2 + 0.5 wt%	15.5	—	—	[70]
CNTs and CFs	0.1 + 0.5 wt%	17.3	—	—	[71]
GNPs	5.0 vol%	32.7	0.78	—	[91]

composites containing other functional fillers. Because more distance is changed between the hybrid GNPs and CNTs. Therefore, more conductive networks are changed. Moreover, owing to the different dimensions of GNPs are with two-dimensional platelets and the CNTs are with one-dimensional tube. More conductive networks in cementitious composites will be composed with synergistic enhancing effects due to the different dimensions, shapes, and ranges. As a result, the cementitious composites incorporating the hybrid GNPs and CNTs in the present article demonstrates the highest stress/strain sensitivities with a lower dosage of the hybrid GNPs and CNTs.

3.3.2 Piezoresistive performance under monotonic compression

Relationships with FCR and monotonic compression of GC0–GC10 from loading to failure after curing 28d are displayed in Figure 23. It can be seen from Figure 23 that the relationships between FCR and stress/strain present a similar development trend. The FCR decreases slowly at first then decreases fastly when increasing stress/strain. Additionally, it increases abruptly when the specimen is withstood the maximum stress. The maximum absolute FCR and stress/strain sensitivities of GC0–GC10 under monotonic compressive load from loading to failure are presented in Figure 24. It shows that the variation rules of the maximum absolute FCR and stress/strain sensitivities of GC0–GC10 under monotonic compression are similar to those of the GC0–GC10 under cyclic compression. The maximum absolute values of FCR and sensitivities vary within the scopes of 8.2–36.0% and 0.01–0.49% MPa^{-1}/18.1–78.2, respectively. Compared with GC0, the scopes of increase rates of GC1–GC10 are 52.2–340.8% and 33.5–390.6%/32.0–332.0%, respectively. The cementitious composites present the largest maximum absolute value of FCR and sensitivities which can reach up to 36.0 and 0.49% MPa^{-1}/78.2, respectively, when the dosage is 5.0 wt%. Comparison of the sensitivities of the composites including nanocarbon functional fillers under monotonic load is shown in Table 4. It can be seen from Table 4 that the FCR under the monotonic compression of the present article is the highest. The results indicate that the composites can be applied to monitor and estimate the health of concrete structures subject to monotonic compression.

4 Conclusions

Cementitious composites incorporating the hybrid GNPs and CNTs with dosage from 0 to 10 wt% with simplified manufacturing methods are developed first. Then, mechanical performances including the relationships between strain and stress, compressive strength, the ultimate strain, and modulus of elasticity are tested. Thereafter, the electrical resistivity is measured using both DC and AC methods under different frequencies. After that, the piezoresistive response withstanding repeated and monotonic compressive load is investigated systematically. Finally, mechanisms of the hybrid GNPs' and CNTs' influence on the performances with cooperation effect are discussed in-depth. Conclusions can be obtained as follows.

1) Mechanical properties of cementitious composites can be enhanced by the hybrid GNPs and CNTs with a dosage of no more than 3.0 wt%. The increased ratios of compressive strength, ultimate strain, and modulus of elasticity are within the ranges of 9.2–31.1%, 2.2–24.4%, and 11.7–46.0%, respectively. However, they decreased within the scopes of 4.8–43.5%, 6.7–11.3%, and 6.5–46.0%, respectively, when the hybrid GNPs and CNTs increase from 4.0 to 10.0 wt%. Moreover, the composites present the maximum and minimum compressive strength/ultimate strain/modulus of elasticity of 108.1 MPa/5,600 με/28.6 GPa, and 46.6 MPa/3,990 με/10.6 GPa, respectively, which corresponds to the hybrid GNPs and CNTs with concentration of 2.0 and 10.0 wt%.

2) The electrical resistivities decrease upon increasing dosage of the hybrid GNPs and CNTs, and the reduction of the electrical resistivities measured by DC and AC methods is achieved in three orders and one order, respectively. In addition, the AC electrical resistivities are decreased with increasing frequencies. Meanwhile, the percolation threshold zone is within the scope of 1.0–6.0 wt%.

3) The electrical resistivity decreases upon increasing the stress/strain, and *vice versa*, presenting stability and reversibility undergoing repeated compression. Additionally, the electrical resistivity is decreased with increasing the load and up surging suddenly under failure conditions to withstand the monotonic compression. Meanwhile, the maximum absolute FCR and stress/strain sensitivities first increase then decrease and almost keep constant at last with increasing the hybrid GNPs and CNTs. Moreover, the composites present the best piezoresistive property containing 5.0 wt% of the hybrid GNPs and CNTs, and the absolute FCR and stress/strain sensitivities corresponding to repeated and monotonic compression reached up to 21.9% and 1.1 % MPa^{-1}/177.9, and 36.0 and 0.49% MPa^{-1}/78.2, respectively. Therefore, stress/strain, cracks, and displacement can be monitored from variations in the electrical properties.

4) Cementitious composites incorporating the hybrid GNPs and CNTs display remarkable electrical conductivities and piezoresistive properties as well as competitive mechanical performances are offered feasibility to explore self-sensing cementitious composites to monitor the health of concrete structures. However, homogeneous dispersion of the hybrid GNPs and CNTs, the relationships between load and FCR withstand dynamic compression, and the self-sensing capability affected by environmental factors must be improved and explored. Therefore, quantity investigations are needed to be conducted in the future.

Funding information: The research is funded by the Excellent Youth Research Project of Hunan Provincial Department of Education (23B0652), the Major Science and Technology Research Project of the China Building Materials Federation (Intrinsic self-sensing concrete for smart full-time and full-area monitoring of major civil infrastructures), the Young Backbone Teachers of Ordinary Universities in Hunan Province of 2023, ([2023], No. 318, documents issued by the Education Department of Hunan Province), the National Science Foundation of China (52368031), the China Postdoctoral Science Foundation (2022M713497), the Jiangxi Provincial Natural Science Foundation (20224BAB204067), the Jiangxi Provincial Department of Transportation Science and Technology Project (2022H0017), the Project of China Construction Engineering Co., Ltd. (CSCEC-2021-Q-56), and the Project of China Construction Second Engineering Bureau Co., Ltd. (2021ZX000004).

Author contributions: All authors have accepted responsibility for the entire content of this manuscript and approved its submission.

Conflict of interest: The authors state no conflict of interest.

References

[1] Dong S, Han B, Ou J, Li Z, Han L, Yu X. Electrically conductive behaviors and mechanisms of short-cut super-fine stainless wire reinforced reactive powder concrete. Cem Concr Compos. 2016;72:48–65.

[2] Zhang L, Ding S, Li L, Dong S, Wang D, Yu X, Han B. Effect of characteristics of assembly unit of CNT/NCB composite fillers on properties of smart cement-based materials. Compos Part A: Appl Sci Manuf. 2018;109:303–20.

[3] Dong S, Li L, Ashour A, Dong X, Han B. Self-assembled 0D/2D nano carbon materials engineered smart and multifunctional cement-based composites. Constr Build Mater. 2021;272:1–14.

[4] Kashif Ur Rehman S, Kumarova S, Ali Memon S, Javed MF, Jameel M. A review of microscale, rheological, mechanical, thermoelectrical and piezoresistive properties of graphene based cement composite. Nanomaterials. 2020;10(10):2076.

[5] Barcelo L, Kline J, Walenta G, Gartner E. Cement and carbon emissions. Mater Struct. 2014;47(6):1055–65.

[6] Ou JP, Li H. Structural health monitoring in mainland China: Review and future trends. Struct Health Monit. 2010;9(3):219–31.

[7] Han BG, Zhang LQ, Ou JP. Smart and multifunctional concrete toward sustainable infrastructures. Berlin: Springer; 2017.

[8] Chung DDL. Self-sensing concrete: From resistance-based sensing to capacitance-based sensing. Int J Smart Nano Mater. 2021;12(1):1–19.

[9] Han BG, Yu Y, Han BZ, Ou JP. Development of a wireless stress/strain measurement system integrated with pressure-sensitive nickel powder-filled cement-based sensors. Sens Actuators A: Phys. 2008;147(2):536–43.

[10] Kashif Ur Rehman S, Ibrahim Z, Memon SA, Jameel M. Nondestructive test methods for concrete bridges: A review. Constr Build Mater. 2016;107:58–86.

[11] Eddib AA, Chung D. First report of capacitance-based self-sensing and in-plane electric permittivity of carbon fiber polymer-matrix composite. Carbon. 2018;140:413–27.

[12] Chung DDL. Cement reinforced with short carbon fibers: a multifunctional material. Compos Part B: Eng. 2000;31(6):511–26.

[13] Banthia N, Djeridane S, Pigeon M. Electrical resistivity of carbon and steel micro-fiber reinforced cements. Cem Concr Res. 1992;22(5):804–14.

[14] Yehia S, Tuan CY, Ferdon D, et al. Conductive concrete overlay for bridge deck deicing: mixture proportioning, optimization, and properties. Mater J. 2000;97(2):172–81.

[15] Chen PW, Chung DDL. Carbon fiber reinforced concrete for smart structures capable of non-destructive flaw detection. Smart Mater Struct. 1993;2(1):22–30.

[16] Baeza FJ, Galao O, Zornoza E, Garcés P. Effect of aspect ratio on strain sensing capacity of carbon fiber reinforced cement composites. Mater & Des. 2013;51:1085–94.

[17] Thomoglou AK, Falara MG, Gkountakou FI, Elenas A, Chalioris CE. Influence of different surfactants on carbon fiber dispersion and the mechanical performance of smart piezoresistive cementitious composites. Fibers. 2022;10(6):49.

[18] Han B, Yu X, Kwon E, Ou J. Effects of CNT concentration level and water/cement ratio on the piezoresistivity of CNT/cement composites. J Compos Mater. 2012;46(1):19–25.

[19] Han BG, Hanb BZ, Ou JP. Experimental study on use of nickel powder-filled Portland cement-based composite for fabrication of piezoresistive sensors with high sensitivity. Sensors and Actuators A: Physical. 2009. 2009;149:51–5.

[20] Han BG, Han BZ, Yu X. Effects of the content level and particle size of nickel powder on the piezoresistivity of cement-based composites/sensors. Smart Mater Struct. 2010;19(6):1–6.
[21] Han B, Zhang K, Yu X, Kwon E, Ou J. Nickel particle-based self-sensing pavement for vehicle detection. Measurement. 2011;44(9):1645–50.
[22] Han B, Wang Y, Sun S, Yu X, Ou J. Nanotip-induced ultrahigh pressure-sensitive composites: Principles, properties and applications. Compos Part A: Appl Sci Manuf. 2014;59(0):105–14.
[23] Zhou G, Yao Y, Lu Z, Yang X, Han J, Wang G, et al. Self-sensing cementitious composites incorporated with botryoid hybrid nanocarbon materials for smart infrastructures. J Intell Mater Syst Struct. 2017;28(6):699–727.
[24] Monteiro AO, Cachim PB, Costa PM. Self-sensing piezoresistive cement composite loaded with carbon black particles. Cem Concr Compos. 2017;81:59–65.
[25] Li H, Xiao HG, Ou JP. Electrical property of cement-based composites filled with carbon black under long-term wet and loading condition. Compos Sci Technol. 2008;68(9):2114–9.
[26] Ozbulut OE, Jiang Z, Harris DK. Exploring scalable fabrication of self-sensing cementitious composites with graphene nanoplatelets. Smart Mater Struct. 2018;27(11):115029.
[27] Abedi M, Fangueiro R, Correia AG. A review of intrinsic self-sensing cementitious composites and prospects for their application in transport infrastructures. Constr Build Mater. 2021;310:125139.
[28] Nalon GH, Lopes Ribeiro JC, Duarte de Araújo EN, Marcio da Silva R, Pedroti LG. Effects of shrinkage-reducing admixtures and expansive agents on the self-sensing behavior of nanomodified cement-based materials. J Build Eng. 2023;78:107648.
[29] Han B, Zheng Q, Sun S, Dong S, Zhang L, Yu X, et al. Enhancing mechanisms of multi-layer graphenes to cementitious composites. Compos Part A: Appl Sci Manuf. 2017;101:143–50.
[30] Bai S, Jiang L, Jiang Y, Jin M, Jiang S, Tao D. Research on electrical conductivity of graphene/cement composites. Adv Cem Res. 2020;32(2):45–52.
[31] Le J, Du H, Dai Pang S. Use of 2D Graphene Nanoplatelets (GNP) in cement composites for structural health evaluation. Compos Part B: Eng. 2014;67:555–63.
[32] Sevim O, Jiang Z, Ozbulut OE. Effects of graphene nanoplatelets type on self-sensing properties of cement mortar composites. Constr Build Mater. 2022;359:129488.
[33] Liu Q, Wu W, Xiao J, Tian Y, Chen J, Singh A. Correlation between damage evolution and resistivity reaction of concrete in-filled with graphene nanoplatelets. Constr Build Mater. 2019;208:482–91.
[34] Dong W, Li W, Zhu X, Sheng D, Shah SP. Multifunctional cementitious composites with integrated self-sensing and hydrophobic capacities toward smart structural health monitoring. Cem Concr Compos. 2021;118:103962.
[35] Guo Y, Li W, Dong W, Wang K, He X, Vessalas K, et al. Self-sensing cement-based sensors with superhydrophobic and self-cleaning capacities after silane-based surficial treatments. Case Stud Constr Mater. 2022;17:e1311.
[36] Liu Q, Xu Q, Yu Q, Gao R, Tong T. Experimental investigation on mechanical and piezoresistive properties of cementitious materials containing graphene and graphene oxide nanoplatelets. Constr Build Mater. 2016;127:565–76.
[37] Liu Q, Gao R, Tam VWY, Li W, Xiao J. Strain monitoring for a bending concrete beam by using piezoresistive cement-based sensors. Constr Build Mater. 2018;167:338–47.
[38] Lu D, Shi X, Wong HS, Jiang Z, Zhong J. Graphene coated sand for smart cement composites. Constr Build Mater. 2022;346:128313.
[39] Dong W, Li W, Sun Z, Ibrahim I, Sheng D. Intrinsic graphene/cement-based sensors with piezoresistivity and superhydrophobicity capacities for smart concrete infrastructure. Autom Constr. 2022;133:103983.
[40] Dong W, Li W, Guo Y, Wang K, Sheng D. Mechanical properties and piezoresistive performances of intrinsic graphene nanoplate/cement-based sensors subjected to impact load. Constr Build Mater. 2022;327:126978.
[41] Han B, Ding S, Yu X. Intrinsic self-sensing concrete and structures: A review. Measurement. 2015;59:110–28.
[42] Li L, Wei H, Hao Y, Li Y, Cheng W, Ismail YA, et al. Carbon nanotube (CNT) reinforced cementitious composites for structural self-sensing purpose: A review. Constr Build Mater. 2023;392:131384.
[43] Yu X, Kwon E. A carbon nanotube/cement composite with piezoresistive properties. Smart Mater Struct. 2009;18(5):1–5.
[44] Konsta-Gdoutos MS, Aza CA. Self sensing carbon nanotube (CNT) and nanofiber (CNF) cementitious composites for real time damage assessment in smart structures. Cem Concr Compos. 2014;53:162–9.
[45] Dong W, Li W, Tao Z, Wang K. Piezoresistive properties of cement-based sensors: Review and perspective. Constr Build Mater. 2019;203:146–63.
[46] Li W, Qu F, Dong W, Mishra G, Shah SP. A comprehensive review on self-sensing graphene/cementitious composites: A pathway toward next-generation smart concrete. Constr Build Mater. 2022;331:127284.
[47] Li W, Dong W, Guo Y, Wang K, Shah SP. Advances in multifunctional cementitious composites with conductive carbon nanomaterials for smart infrastructure. Cem Concr Compos. 2022;128:104454.
[48] Ramezani M, Kim YH, Sun Z. Modeling the mechanical properties of cementitious materials containing CNTs. Cem Concr Compos. 2019;104:103347.
[49] Yoo DY, You I, Youn H, Lee SJ. Electrical and piezoresistive properties of cement composites with carbon nanomaterials. J Compos Mater. 2018;52(24):3325–40.
[50] You I, Yoo DY, Kim S, Kim MJ, Zi G. Electrical and self-sensing properties of ultra-high-performance fiber-reinforced concrete with carbon nanotubes. Sensors. 2017;17(11):2481.
[51] Jianlin L, Kwok L C, Qiuyi L, Shunjian C, Lu L, Dongshuai H, Chunwei Z. Piezoresistive properties of cement composites reinforced by functionalized carbon nanotubes using photo-assisted Fenton. Smart Mater Struct. 2017;26(3):35025.
[52] Nam IW, Souri H, Lee H. Percolation threshold and piezoresistive response of multi-wall carbon nanotube/cement composites. Smart Struct Syst. 2016;18(2):217–31.
[53] Materazzi AL, Ubertini F, Alessandro DA Carbon nanotube cement-based transducers for dynamic sensing of strain. Cem Concr Compos. 2013;37:2–11.
[54] Saafi M. Wireless and embedded carbon nanotube networks for damage detection in concrete structures. Nanotechnology. 2009;20(39):1–7.
[55] Han B, Zhang K, Yu X, Kwon E, Ou J. Electrical characteristics and pressure-sensitive response measurements of carboxyl MWNT/cement composites. Cem Concr Compos. 2012;34(6):794–800.
[56] D'Alessandro A, Tiecco M, Meoni A, Ubertini F. Improved strain sensing properties of cement-based sensors through enhanced carbon nanotube dispersion. Cem Concr Compos. 2021;115:103842.

[57] Deng S, Fan J, Li G, Zhang M, Li M. Influence of styrene-acrylic emulsion additions on the electrical and self-sensing properties of CNT cementitious composites. Constr Build Mater. 2023;403:133172.
[58] Chuah S, Pan Z, Sanjayan JG, Wang CM, Duan WH. Nano reinforced cement and concrete composites and new perspective from graphene oxide. Constr Build Mater. 2014;73:113–24.
[59] D'Alessandro A, Rallini M, Ubertini F, Materazzi AL, Kenny JM. Investigations on scalable fabrication procedures for self-sensing carbon nanotube cement-matrix composites for SHM applications. Cem Concr Compos. 2016;65:200–13.
[60] Ramezani M, Dehghani A, Sherif MM. Carbon nanotube reinforced cementitious composites: A comprehensive review. Constr Build Mater. 2022;315:125100.
[61] Ramezani M, Kim YH, Sun Z, Sherif MM. Influence of carbon nanotubes on properties of cement mortars subjected to alkali-silica reaction. Cem Concr Compos. 2022;131:104596.
[62] Ding Y, Chen Z, Han Z, Zhang Y, Pacheco-Torgal F. Nano-carbon black and carbon fiber as conductive materials for the diagnosing of the damage of concrete beam. Constr Build Mater. 2013;43:233–41.
[63] Ramezani M, Kim YH, Sun Z. Mechanical properties of carbon-nanotube-reinforced cementitious materials: Database and statistical analysis. Mag Concr Res. 2020;72(20):1047–71.
[64] Ding S, Wang YW, Ni YQ, Han B. Structural modal identification and health monitoring of building structures using self-sensing cementitious composites. Smart Mater Struct. 2020;29(5):55013.
[65] Azhari F, Banthia N. Cement-based sensors with carbon fibers and carbon nanotubes for piezoresistive sensing. Cem Concr Compos. 2012;34(7):866–73.
[66] Wang Y, Zhang L. Development of self-sensing cementitious composite incorporating hybrid graphene nanoplates and carbon nanotubes for structural health monitoring. Sens Actuators A: Phys. 2022;336:113367.
[67] Belli A, Mobili A, Bellezze T, Tittarelli F, Cachim P. Evaluating the self-sensing ability of cement mortars manufactured with graphene nanoplatelets, virgin or recycled carbon fibers through piezoresistivity tests. Sustainability. 2018;10(11):4013.
[68] Jawed Roshan M, Abedi M, Gomes Correia A, Fangueiro R. Application of self-sensing cement-stabilized sand for damage detection. Constr Build Mater. 2023;403:133080.
[69] Liu L, Xu J, Yin T, Wang Y, Chu H. Improved conductivity and piezoresistive properties of Ni-CNTs cement-based composites under magnetic field. Cem Concr Compos. 2021;121:104089.
[70] Thomoglou AK, Falara MG, Voutetaki ME, Fantidis JG, Tayeh BA, Chalioris CE. Electromechanical properties of multi-reinforced self-sensing cement-based mortar with MWCNTs, CFs, and PPs. Constr Build Mater. 2023;400:132566.
[71] Thomoglou AK, Falara MG, Gkountakou FI, Elenas A, Chalioris CE. Smart cementitious sensors with nano-, micro-, and hybrid-modified reinforcement: mechanical and electrical properties. Sensors. 2023;23(5):2405.
[72] Guo Y, Li W, Dong W, Luo Z, Qu F, Yang F, et al. Self-sensing performance of cement-based sensor with carbon black and polypropylene fibre subjected to different loading conditions. J Build Eng. 2022;59:105003.
[73] Pan HH, Lai TZ, Chaipanich A, Wittinanon T. Effect of graphene on the piezoelectric properties of cement-based piezoelectric composites. Sens Actuators A: Phys. 2022;346:113882.
[74] Tao J, Wang X, Wang Z, Zeng Q. Graphene nanoplatelets as an effective additive to tune the microstructures and piezoresistive properties of cement-based composites. Constr Build Mater. 2019;209:665–78.
[75] Ding S, Wang X, Han B. New-generation cement-based nanocomposites with in-situ grown CNT on cement. New-Generation Cement-Based Nanocomposites. Singapore: Springer; 2023. p. 241–61
[76] Ma PC, Siddiqui NA, Marom G, Kim JK. Dispersion and functionalization of carbon nanotubes for polymer-based nanocomposites: A review. Compos Part A: Appl Sci Manuf. 2010;41(10):1345–67.
[77] Mingqing S, Zhuoqiu L, Qizhao M, Darong S. A study on thermal self-monitoring of carbon fiber reinforced concrete. Cem Concr Res. 1999;29(5):769–71.
[78] ASTM C1202: Standard test method for electrical indication of concrete's ability to resist chloride ion penetration. West Conshohocken, PA, United States: ASTM International, 2019.
[79] Suchorzewski J, Prieto M, Mueller U. An experimental study of self-sensing concrete enhanced with multi-wall carbon nanotubes in wedge splitting test and DIC. Constr Build Mater. 2020;262:120871.
[80] Standard Test Method for Compressive Strength of Hydraulic Cement Mortars. USA, Astm, 2020.
[81] Han B, Zhang L, Zeng S, Dong S, Yu X, Yang R, et al. Nano-core effect in nano-engineered cementitious composites. Compos Part A: Appl Sci Manuf. 2017;95:100–9.
[82] Han B, Zhang L, Sun S, Yu X, Dong X, Wu T, et al. Electrostatic self-assembled carbon nanotube/nano carbon black composite fillers reinforced cement-based materials with multifunctionality. Compos Part A: Appl Sci Manuf. 2015;79:103–15.
[83] Ghazizadeh S, Duffour P, Skipper NT, Bai Y. Understanding the behaviour of graphene oxide in Portland cement paste. Cem Concr Res. 2018;111:169–82.
[84] Lavagna L, Musso S, Ferro G, et al. Cement-based composites containing functionalized carbon fibers. Cem Concr Compos. 2018;88:165–71.
[85] Musso S, Tulliani JM, Ferro G, Tagliaferro A. Influence of carbon nanotubes structure on the mechanical behavior of cement composites. Compos Sci Technol. 2009;69(11):1985–90.
[86] ASTM C469. Standard Test Method for Static Modulus of Elasticity and Poisson's Ratio of Concrete in Compression. USA, 2002.
[87] Ozbulut OE, Jiang Z, Harris DK. Exploring scalable fabrication of self-sensing cementitious composites with graphene nanoplatelets. Smart Mater Struct. 2018;27(11):1–18.
[88] Yoo D, You I, Lee S. Electrical properties of cement-based composites with carbon nanotubes, graphene, and graphite nanofibers. Sensors. 2017;17(5):1064.
[89] Han BG, Ding SQ, Yu X. Intrinsic self-sensing concrete and structures: A review. Measurement. 2015;59:110–28.
[90] Sun S, Han B, Jiang S, Yu X, Wang Y, Li H, et al. Nano graphite platelets-enabled piezoresistive cementitious composites for structural health monitoring. Constr Build Mater. 2017;136:314–28.
[91] Sun S, Ding S, Han B, Dong S, Yu X, Zhou D, et al. Multi-layer graphene-engineered cementitious composites with multifunctionality/intelligence. Compos Part B: Eng. 2017;129:221–32.
[92] Dong W, Li W, Luo Z, Long G, Vessalas K, Sheng D. Structural response monitoring of concrete beam under flexural loading using smart carbon black/cement-based sensors. Smart Mater Struct. 2020;29(6):65001.